

1 **Water restrictions under climate change: a Rhone-** 2 **Mediterranean perspective combining ‘bottom up’ and ‘top-** 3 **down’ approaches**

4 Eric SAUQUET¹, Bastien RICHARD^{1,2}, Alexandre DEVERS¹, Christel PRUDHOMME^{3,4,5}

5

Correspondance to: E. Sauquet (eric.sauquet@irstea.fr)

6 ¹ Irstea, UR Riverly, 5 rue de la Doua CS20244, 69625 Villeurbanne cedex, France

7 ² Irstea, UMR G-EAU, Water resource management, Actors and Uses Joint Research Unit, Campus Agropolis -
8 361 rue Jean-François Breton – BP 5095, 34196 Montpellier Cedex 5, France

9 ³ European Centre for Medium-Range Weather Forecasts, Reading, UK

10 ⁴ Department of Geography, Loughborough University, Loughborough, LE11 3TU, UK

11 ⁵ NERC Centre for Ecology & Hydrology, Maclean Building, Benson Lane, Crowmarsh Gifford, Wallingford,
12 Oxon, OX10 8BB, UK

13 **Abstract** Drought management plans (DMPs) require an overview of future climate conditions for ensuring long-
14 term relevance of existing decision-making processes. To that end, impact studies are expected to best reproduce
15 decision-making needs linked with catchment intrinsic sensitivity to climate change. The objective of this study is
16 to apply a risk-based approach through sensitivity, exposure and performance assessments to identify where and
17 when, due to climate change, access to surface water constrained by legally-binding water restrictions may
18 question agricultural activities. After inspection of legally-binding water restrictions (WR) from the DMPs in the
19 Rhône-Méditerranée (RM) district, a framework to derive WR durations was developed based on harmonized low-
20 flow indicators. Whilst the framework could not perfectly reproduce all WR ordered by state services, as deviations
21 from socio-political factors could not be included, it enabled to identify most WRs under current baseline, and to
22 quantify the sensitivity of WR duration to a wide range of perturbed climates for 106 catchments. Four classes of
23 responses were found across the RM district. The information provided by the national system of compensation to
24 farmers during the 2011 drought was used to define a critical threshold of acceptable WR, related to the current
25 activities over the RM district. The study finally concluded that catchments in mountainous areas, highly sensitive
26 to temperature changes, are also the most predisposed to future restrictions under projected climate changes
27 considering current DMPs, whilst catchments around the Mediterranean Sea were found mainly sensitive to
28 precipitation changes and irrigation use was less vulnerable to projected climatic changes. The tools developed

29 enable a rapid assessment of the effectiveness of current DMPs under climate change, and can be used to prioritize
30 review of the plans for those most vulnerable basins.

31 **Keywords** Climate change; drought management plan; low-flow; France; scenario-neutral approach; response
32 surface; vulnerability; water restriction.

33 **1 Introduction**

34 The Mediterranean region is known as one of the “hot spots” of global change (Giorgi 2006; Paeth *et al.* 2017)
35 where environmental and socio-economic impacts of climate change and human activities are likely to be very
36 pronounced. The intensity of the changes is still uncertain, however, climate models agree on significant future
37 increase in frequency and intensity of meteorological, agricultural and hydrological droughts in Southern Europe
38 (Jiménez Cisneros *et al.* 2014; Touma *et al.* 2015), with climate change likely to exacerbate the variability of
39 climate with regional feedbacks affecting Mediterranean-climate catchments (Kondolf *et al.* 2013). Facing more
40 severe low-flows and significant losses of snowpack, southeastern France will be subject to substantial alterations
41 of water availability: Chauveau *et al.* (2013) have shown a potential increase in low-flow severity by the 2050’s
42 with a decrease in low-flow statistics to 50% for the Rhône River near its outlet. Andrew and Sauquet (2017) have
43 reported that global change will most likely result in a decrease in water resources and an increase both in pressure
44 on water resources and in occurrence of periods of water limitation within the Durance River basin, one of the
45 major water tower of southeastern France. In addition, Sauquet *et al.* (2016) have suggested the need to open the
46 debate on a new future balance between the competing water uses. More recently, based on climate projections
47 obtained from Coupled Model Intercomparison Project Phase 5 (Taylor *et al.* 2012), Dayon *et al.* (2018) have
48 shown a significant increase in hydrological drought severity with a meridional gradient (up to -55% in southern
49 France for both the annual minimum monthly flow with a return period of 5 years and the mean summer river
50 flow) while a more uniform increase in agricultural drought severity is projected over France for the end of the
51 21st century.

52 The challenges associated with possible impact of climate change on droughts have received increasing attention
53 by researchers, stakeholders and policy makers in the last decades. To date climate change impact studies are
54 usually dedicated to water resources (e.g., Vidal *et al.* 2016, Collet *et al.* 2018, Hellwig and Stahl 2018, Samaniego
55 *et al.* 2018) or water needs for the competing users (e.g., Bisselink *et al.* 2018). However, examining the suitability
56 of regulatory instruments, such as Drought Management Plans, is also essential to establish successful adaptation

57 strategies. These plans state which type of water restrictions should be imposed to non-priority uses during severe
58 low-flow events; under climate change, those water restrictions and stakeholders' access to water resources might
59 need to be revised as drought patterns and severity might change. In most climate change impact studies, analyses
60 on the regulatory measures are often limited to maintaining environmental flows – especially when assessing future
61 hydropower potential. To date, no climate change impact on water regulatory measures have yet been assessed at
62 the regional scale, highlighting a gap in developing robust adaptation plans. This study aims to address this gap by
63 suggesting a framework, applying it to southeastern France and publishing the associated results.

64 The paper develops a framework to simulate legally-binding water restrictions (WR) under climate change in
65 the Rhone-Méditerranée district (southeastern France) and to assess the likelihood of future restrictions depending
66 on their sensitivity, performance and exposure to climate deviations. The approach is adapted from the risk-based
67 approaches such as developed in parallel by Brown *et al.* (2011) –named “Decision Tree Framework” –and
68 Prudhomme *et al.* (2010) –named “Scenario neutral approach”–and aims to establish a ranking of areas vulnerable
69 to climate change in terms of water access for agricultural uses . This research is a scientific contribution to the
70 ongoing decade 2013–2022 entitled “Panta Rhei – Everything Flows” initiated by the International Association of
71 Hydrological Sciences and more specifically to the “Drought in the Anthropocene” working group
72 ([https://iahs.info/Commissions--W-Groups/Working-Groups/Panta-Rhei/Working-Groups/Drought-in-the-](https://iahs.info/Commissions--W-Groups/Working-Groups/Panta-Rhei/Working-Groups/Drought-in-the-Anthropocene.do)
73 [Anthropocene.do](https://iahs.info/Commissions--W-Groups/Working-Groups/Panta-Rhei/Working-Groups/Drought-in-the-Anthropocene.do), Van Loon *et al.* 2016). Legally-binding water restrictions and their associated decision-making
74 processes are important for the blue water footprint assessment at the catchment scale.

75 The paper is organized in four parts. Sect. 2 introduces the area of interest and the source of data. Sect. 3 is a
76 synthesis of the mandatory processes for managing drought condition implemented within the Rhône-Méditerranée
77 district and the related water restriction orders adopted over the period 2005-2016. Sect. 4 describes the general
78 modelling framework developed to simulate WR decisions. The approach is implemented at both local and
79 regional scales and results discussed in Sect. 5 before drawing general conclusions in Sect. 6.

80 **2 Study area and materials**

81 **2.1 Study area**

82 The Rhone-Méditerranée district covers all the Mediterranean coastal rivers and the French part of the Rhône
83 River basin, from the outlet of Lake Geneva to its mouth (Fig. 1). Climate is rather varied with a temperate
84 influence in the north, a continental influence in the mountainous areas and a Mediterranean climate with dry and

85 hot summers dominating in the south and along the coast. In the mountainous part (in both the Alps and the
86 Pyrenees) the snowmelt-fed regimes are observed in contrast to the northern part under oceanic climate influences,
87 where seasonal variations of evaporation and precipitation drive the monthly runoff pattern (Sauquet *et al.* 2008).

88 Water is globally abundant but unevenly between the mountainous areas, the northern and southern parts of the
89 Rhône-Méditerranée (RM) district and water resources are under high pressure due to water abstractions. For the
90 period 2008-2013, annual total water withdrawal was around 6 billion of m³ in the (excluding any water abstraction
91 for energy such as cooling nuclear plants and hydropower) with a more than used for irrigation (3.4 billion of m³,
92 including 2 billion of m³ for channel conveyance). Use for public and industrial supply is of 1.6 and 1 billion of
93 m³, respectively. Because of an intense competition for water between different users — agricultural, municipal,
94 and industrial — and the environment, some areas within the RM district can be vulnerable during low-flow
95 periods. Around 40% of the RM district suffers from water stress and scarcity ([http://www.rhone-](http://www.rhone-mediterranee.eaufrance.fr/gestion/gestion-quantite/problematique.php)
96 [mediterranee.eaufrance.fr/gestion/gestion-quantite/problematique.php](http://www.rhone-mediterranee.eaufrance.fr/gestion/gestion-quantite/problematique.php)) and has been identified by the French RM
97 Water Agency as areas with persistent imbalance between water supply and water demand.

98 **2.2 Drought management plan**

99 Drought management plans (DMPs) define specific actions to be undertaken to enhance preparedness and
100 increase resilience to drought. In France DMPs include regulatory frameworks to be applied in case of drought,
101 named “arrêtés cadres sécheresse”. The past and operating DMPs and the water restriction orders were inspected
102 in the 28 departments of the RM district. They were obtained from:

- 103 - The database of the DREAL Auvergne-Rhône-Alpes (“Direction Régionale de l’Eau, de l’Alimentation et du
104 Logement” in French) including WR levels and duration at the catchment scale available over the period 2005-
105 2016 within the RM district;
- 106 - The online national database PROPLUVIA (<http://propluvia.developpement-durable.gouv.fr>) with WR levels
107 and dates of adoption at the catchment scale for the whole France available from 2012.

108 The most recent consulted documents date from January 2017.

109 **2.3 Hydrological data**

110 The hydrological observation dataset is a subset of the 632 French near-natural catchments identified by
111 Caillouet *et al.* (2017). Daily flow data from 1958 to 2013 were extracted from the French HYDRO database
112 (<http://hydro.eaufrance.fr/>). Time series with more than 30% of missing values or more than 30% of null values

113 were disregarded. Finally, the total dataset consist of 106 gauged catchments located in the RM district with minor
114 human influence and with high quality data. The selected catchments are benchmark catchments where near natural
115 drought events are observed and current water availability is monitored. Water can be abstracted from other nearby
116 streams.

117 A selection of 15 evaluation catchments (Table 1) were used to calibrate and to evaluate the Water Restriction
118 Level modelling framework (Sect. 4), selected because (i) they have complete records of stated water restriction,
119 including dates and levels of restrictions - which was not the case of other catchments, and (ii) they are located in
120 areas where water restriction decisions are frequent. To facilitate interpretation, the 15 catchments have been
121 ordered along the north-south gradient. The Ouche and Argens River basins (n°1 and 15 in Table 1) are the
122 northernmost and the southernmost gauged basins, respectively. The 15 catchments encompass a large variety of
123 river flow regimes according to the classification suggested by Sauquet *et al.* (2008) (see Appendix A) that can be
124 observed in the RM district (e.g., the Ouche (1 in Table 1, pluvial regime), Roizonne (3, transition regime) and
125 Argens (15, snowmelt-fed regime) River basins).

126 **2.4 Climate data**

127 Baseline climate data were obtained from the French near-surface Safran meteorological reanalysis (Quintana-
128 Seguí *et al.* 2008; Vidal *et al.* 2010) onto an 8-km resolution grid from 1 August 1958 to 2013. Exposure data was
129 based on the regional projections for France (Table 2) available from the DRIAS French portal ([www.drias-](http://www.drias-climat.fr)
130 [climat.fr](http://www.drias-climat.fr), Lémond *et al.* 2011). Catchment-scale data were computed as weighted mean for temperature and sum
131 for precipitation based on the river network elaborated by Sauquet (2006).

132 **3 Operating Drought Management Plans in the Rhône-Méditerranée district**

133 The French Water Act amended on September 24, 1992 (decree n°92/1041) defines the operating procedures for
134 the implementation of drought management plan (DMP). Following the 2003 European heat wave, drought
135 management plans including water restrictions have been gradually implemented in France (MEDDE 2004). Water
136 restrictions fall within the responsibility of the prefecture (one per administrative unit or department), as mentioned
137 in article L211-3 II-1° of the French environmental code. Their role in drought management is to ensure that
138 regulatory approvals for water abstraction continuously meet the balance between water resource availability and
139 water uses including needs for aquatic ecosystems. *De facto*, legally-binding water restrictions have to fulfill three
140 principles: (i) being gradually implemented at the catchment scale in regard with low-flow severity observed at

141 various reference locations, (ii) ensuring users equity and upstream-downstream solidarity and (iii) being time-
142 limited to fix cyclical deficits rather than structural deficits. The prefecture is in charge of establishing and
143 monitoring the DMP operating in the related department.

144 Past and current drought management plans were analyzed to identify the past and current modalities of
145 application, the frequency of water restriction orders and the areas affected by water restrictions. Gathering and
146 studying the regulatory documents was a tedious in particular because of their lack of clear definition of the
147 hydrological variables used in the decision-making process.

148 This analysis shows that the implementation of the DMPs has evolved for many departments since 2003, e.g.,
149 with changes in the terminology and a national scale effort to standardize WR levels. Now severity in low-flows
150 is classified into four levels, which are related to incentive or legally-binding water restrictions. These measures
151 affect recreational uses, vehicle washing, lawn watering and domestic, irrigation and industrial uses (Table 3).
152 Level 0 (named “vigilance”) refers to incentive measures, such as awareness campaign to promote low water
153 consumption from public bodies and general public. Levels 1 to 3 are incrementally legally-binding restriction
154 levels; level 1 (named “alert”) and 2 (named “reinforced alert”) enforcing reductions in water abstraction for
155 agriculture uses, or several days a week of suspension; level 3 (named “crisis”) involves a total suspension of water
156 abstraction for non-priority uses, including abstraction for agricultural uses and home gardening, and authorizes
157 only water abstraction for drinking water and sanitation services. Due to change in the naming of WR levels since
158 their creation one task was dedicated to restate the WR decisions (hereafter “OBS”) since 2005 with respect to the
159 current classification into four WR levels.

160 For all catchments, a WR decision chronology was derived, showing a large spatial variability in WR (Fig. 1) -
161 note that the 15 evaluation catchments (Table 1) are located in the most affected areas. Between 2005 and 2012,
162 WR decisions were mainly adopted between April and October (98% of the WR decisions, Fig. 2), with 62% in
163 July or August, peaking in July.

164 Decisions for adopting, revoking or upgrading a WR measure are taken after consultation of “drought
165 committees” bringing the main local stakeholders together, the meeting frequency of which is irregular and
166 depends on hydrological drought development. The adopted restriction level is mainly based on the existing
167 hydrological conditions at the time, *i.e.*, based on low-flow monitoring indicators measured at a set of reference

168 gauging stations and their departure from a set of regulatory thresholds. This varies greatly across the RM district
169 (Fig. 3). The low-flow monitoring indicators usually considered are:

- 170 - the daily discharge Q_{daily} ,
- 171 - the maximum discharge QCd , for a window with length d days, $QCd(t)=\max(Q_{daily}(t'), t' \in [t-d+1, t])$ and
- 172 - the mean discharge VCd , for a window with length d days, $VCd(t)=\frac{1}{d} \int_{t-d+1}^t Q_{daily}(t') dt'$.

173 Both QCd and VCd are computed over the whole discharge time series on moving time windows with duration
174 d associated with WR decision varying between 2 and 10 days depending on DMPs. $VC3$ (40% of DMPs) and
175 $QC7$ (17% of DMPs) are the most commonly used, but other single indicators include Q_{daily} (17%), $QC5$ (14%),
176 $QC10$ (8%), $QC2$ (3%), $VC10$ (3%), and with mixed indicators also used (e.g., 14% of $VC3$ and Q_{daily} together).

177 The threshold associated with WR also varies within the district, generally associated with statistics derived
178 from low-flow frequency analysis, but also fixed to locally-defined ecological requirements. In the context of
179 DMPs, series of minimum QCd or VCd are calculated by the block minima approach and thereafter fitted to a
180 statistical distribution. The block is not the year but the month or given by the division of the year into 37 10-
181 day time-window. The regulatory thresholds are given by quantiles with four different recurrence intervals
182 associated to the four restriction levels. Generally, return periods T of 2, 5, 10 and 20 years are associated with
183 the “vigilance”, “alert”, “reinforced alert” and “crisis” restriction levels, respectively. For example, let us
184 consider thresholds based on the annual monthly minima of $VCNd$. The block minima approach is carried out
185 on the N years of records for each month i , $i=1, \dots, 12$ leading to twelve datasets $\{\min\{VCNd(t), month(t)=i,$
186 $year(t)=j\}, j=1, \dots, N\}$. The twelve fitted distribution allows the calculation of 48 values of thresholds (=12
187 months \times 4 levels) with four T -year recurrence intervals.

188 The meteorological situation is also examined in terms of precipitation deficit and likelihood of significant
189 rainfall event considering available short to medium-range weather forecasts. There are heterogeneities in the
190 drought monitoring variables, the time period on which deficit is calculated and the permissible deviation from
191 long term average values.

192 Where appropriate, other supporting local observations such as groundwater levels, reservoir water levels,
193 field surveys provided by the ONDE network (Beaufort *et al.* 2018) or feedbacks from stakeholders can be used
194 to inform final decisions.

195 Since their creation, DMPs have been frequently updated regarding the definition of the regulatory thresholds
196 and the monitoring variables, the water uses affected by legally-binding restrictions, the selection of the monitoring
197 sites, etc. It was especially done following the publication of the circular of the French ministry of Ecology in May
198 2011, and updates often occur after a year with a severe drought to include feedbacks and lessons for the future.
199 Decision-making processes is definitely heterogeneous in both time and space, which does not make the WR
200 modelling easy. In addition, official texts stating the DMPs were not all available for this study. Facing this
201 complexity, simplifying assumptions will be considered in the modelling framework presented in Section 4.3.4
202 Risk-based framework and the related tools.

203 **3 Risk-based framework and the related tools**

204 **4.1 The scenario neutral concept**

205 Traditionally, hydrological impact studies are often based on “top down” (scenario-driven) approaches, easy to
206 interpret, but with associated conclusions becoming outdated as new climate projections are produced. In addition
207 scenario-based studies may fail to match decision-making needs since the implication in terms of water
208 management is usually ignored (Mastrandrea *et al.* 2010). As a substitute to scenario-driven approach, the
209 scenario-neutral approach (Brekke *et al.* 2009, Prudhomme *et al.* 2010, 2013a, 2013b, 2015, Brown *et al.* 2012,
210 Brown and Wilby 2012, Culley *et al.* 2016, Danner *et al.* 2017) has been developed to better address risk-based
211 decision issues. The suggested framework shifts the focus on the current vulnerability of the system affected by
212 changes and on critical thresholds above which the system starts to fail to identify possible maladaptation strategies
213 (Broderick *et al.* 2019). Applied to water management issues, the scenario-neutral studies (Weiß 2011, Wetterhall
214 *et al.* 2011, Brown *et al.* 2011, Whateley *et al.* 2014) aim at improving the knowledge of the system’s vulnerability
215 to changes and at bridging the gap between scientists and stakeholders facing needs in relevant adaptation strategy.
216 Prudhomme *et al.* (2010) have suggested combining of the sensitivity framework with ‘top-down’ projections
217 through climate response surfaces. This approach has been applied to low-flows in the UK (Prudhomme *et al.*
218 2015) and its interests have been discussed as a support tool for drought management decisions.

219 The risk-based framework adopted contains three independent components (Fig. 4):

- 220 (i) Sensitivity analysis (Fronzek *et al.* 2010) based on simulations under a large spectrum of perturbed
221 climates to (a) quantify how policy-relevant variables respond to changes in different climate factors,
222 and (b) identify the climate factors to which the system is the most sensitive. Addressing (a) and (b)

223 may help modelers to check the relevance of their model (e.g., unexpected sensitivity to a climate factor
224 regarding the know processes influencing the rainfall-runoff transformation). From an operational
225 viewpoint, it may encourage stakeholders to monitor in priority the variables that affect the system of
226 interest (reinforcement of the observation network, literature monitoring, etc.),

227 (ii) Sustainability or performance assessment, aiming to identify under which climate (or other) conditions
228 (e.g., no rain period in spring, heat wave in summer, etc.) the system fails. A key-challenge in bottom-
229 up framework is to define performance metrics and associated critical thresholds relevant for the system
230 of interest. In the case of our study, these thresholds will make it possible to distinguish duration of
231 water restrictions, which are unacceptable for users,

232 (iii) Exposure, as defined by state-of-the-art regional climate trajectories superimposed to the climate
233 response surface. The exposure measures the probability of changes occurring for different lead times
234 based on available regional projections.

235 All the components of the framework together contribute to the vulnerability of the system (including its
236 management) to systematic climatic deviations.

237 The sensitivity analysis was conducted applying a water restriction modelling framework. Climate conditions
238 were generated applying incremental changes to historical data (precipitation and temperature) and introduced as
239 inputs in the developed models to derive occurrence and severity of water restriction under modified climates. The
240 tool chosen here to display the interactions between water restriction and the parameters that reflect the climate
241 changes is a two-dimensional response surface, with axes represented by the main climate drivers. This
242 representation is commonly used in scenario neutral approach. For example, in both Culley *et al.* (2016) and Brown
243 *et al.* (2012) the two axes were defined by the changes in annual precipitation and temperature. When changes
244 affect numerous attributes of the climate inputs, additional analyses (e.g., elasticity concept combined with
245 regression analysis (Prudhomme *et al.* 2015), Spearman rank correlation and Sobol' sensitivity analyses (Guo *et*
246 *al.* 2017)) may be required to point out the key variables with the largest influence on water restriction that form
247 thereafter the most appropriate axes for the response surfaces.

248 Performance assessment is a challenging task for hydrologists since it requires information on the impact of
249 extreme hydrometeorological past events on stakeholders' activities. Simonovic (2010) used observed past events
250 selected with local authorities on a case study in southwestern Ontario (Canada), chosen for their past impact
251 (flood peak associated with a top-up of the embankments of the main urban center; level II drought conditions of

252 the low water response plan). Schlef *et al.* (2018) set the threshold to the worst modelled event under current
253 conditions. Whateley *et al.* (2014) assessed the robustness of a water supply system and the threshold is fixed to
254 the cumulative cost penalties due to water shortage evaluated under the current conditions. Brown *et al.* (2012)
255 and Ghile *et al.* (2014) suggested selecting thresholds according to expert-judgment of unsatisfactory performance
256 of the system by stakeholders, whilst Ray and Brown (2015) use results from benefit-cost analyses. The spatial
257 coverage of a large area, such as the RM district, and the heterogeneity in water use (domestic needs, hydropower,
258 recreation, irrigation, etc.) makes it challenging for a systematic, consistent and comparable stakeholder
259 consultation to be conducted and for a relevant critical threshold T_c to be fixed for all the users. Facing this
260 complexity, only the irrigation water use will be examined here, since it is the sector which consumes most
261 water at the regional scale, with a critical threshold defined for this single water use.

262 Exposure to changes here is measured using regional projections, visualized graphically by positioning the
263 regional projections in the coordinate system of the climate response surfaces and identifying the associated
264 likelihood of failure relative to T_c . Note that, to update the risk assessment, only the exposure component has to
265 be examined (including the latest climate projections available onto the response surfaces).

266 **4.2 The rainfall-runoff modelling**

267 The conceptual lumped rainfall-runoff model GR6J was adopted for simulating daily discharge at 106 selected
268 catchments of the RM district. The GR6J model is a modified version of GR4J originally developed by Perrin *et al.*
269 *et al.* (2003), well suited to simulate low-flow conditions (Pushpalatha *et al.* 2011). The 4-parameter version of the
270 model GR4J has been progressively modified. Lemoine (2008) has suggested a new groundwater exchange
271 function and a new routing store representing long-term memory in the GR5J model. Pushpalatha *et al.* (2011)
272 finally introduced in the GR6J model an exponential store in parallel to the existing store of the GR5J model.
273 Considering additional routing stores is consistent regarding the natural complexity of hydrological processes, and
274 in particular, the dynamics of flow components in low flows (Jakeman *et al.*, 1990).

275 The GR6J model has six parameters to be fitted (Fig. 5): the capacity of soil moisture reservoir (X1) and of the
276 routing reservoir (X3), the time base of a unit hydrograph (X4), two parameters of the groundwater exchange
277 function F (X2 and X5) and a coefficient for emptying exponential store (X6). The GR6J model is combined here
278 with the CemaNeige semi-distributed snowmelt runoff component (Valéry *et al.* 2014). The catchment is divided
279 into five altitudinal bands of equal area on which snowmelt and snow accumulation processes are represented. For

280 each band, daily meteorological inputs – including solid fractions of precipitation - are extrapolated using elevation
281 as covariate and the snow routine is calculated separately. Finally, its outputs are then aggregated at the catchment
282 scale to feed GR6J. The two parameters of CemaNeige S1 and S2 control the snowpack inertia and the snowmelt,
283 respectively. S1 is used to compute the thermal state of the snow pack eTG , which is an equivalent to the internal
284 snowpack temperature ($^{\circ}\text{C}$). $eTG(t)$ at day t is a weighted linear combination of the value of $eTG(t-1)$ ($\times S1$) and
285 the air temperature at the day t ($\times(1-S1)$). S2 is the snowmelt degree-day factor used to calculate the daily snowmelt
286 depth by multiplying the air temperature when it exceeds 0°C , with S2. The splitting coefficient of effective rainfall
287 between the two stores (SC, in Fig. 5) has been fixed to 0.4 by Pushpalatha *et al.* (2011) since calibrating SC lead
288 to only slight better performance. The allocation of the outflow from the soil moisture reservoir in 90% as
289 percolation and 10% as surface and sub-surface runoff in the GR6J model is the results of previous studies. The
290 GR6J model was selected for its good performance across a large spectrum of river flow regimes (e.g., Hublart *et*
291 *al.* 2016, Poncelet *et al.* 2017).

292 No routine to simulate water management (e.g., reservoir) was considered here since discharges of the 106
293 gauging stations are weakly altered by human actions or naturalized discharges (*i.e.* flows corrected from the
294 effects of water use). The eight parameters (six from the GR6J model and two from the CemaNeige module) were
295 calibrated against the observed discharges using the baseline Safran reanalysis as input data and the Kling–Gupta
296 efficiency criterion (Gupta *et al.* 2009) KGE_{SQRT} calculated on the square root of the daily discharges as objective
297 function. The KGE_{SQRT} criterion was used to give less emphasis of extreme flows (both low and high flows). As
298 the climate sensitivity space includes unprecedented climate conditions (including colder climate conditions
299 around the current-day condition), the CemaNeige module was run for all the 106 catchments even for those not
300 currently influenced by snow.

301 The two step procedure suggested by Caillouet *et al.* (2017) was adopted for the calibration: first the eight free
302 parameters were fitted only for the catchments significantly influenced by snowmelt processes – *i.e.*, when the
303 proportion of snowfall to total precipitation $> 10\%$ - and second, for the other catchments, the medians of the
304 CemaNeige parameters were fixed and the six remaining parameters are then calibrated. Calibration is carried out
305 over the period 1 January 1973 to 30 September 2006 with a 3-year spin-up period to limit the influence of reservoir
306 initialization on the calibration results. The criterion KGE_{SQRT} and the Nash-Sutcliffe efficiency criterion on the
307 log transformed discharge NSE_{LOG} (Nash and Sutcliffe 1970) were calculated over the whole period 1958-2013
308 for the subset of 15 evaluation catchments (Table 1), showing KGE_{SQRT} and NSE_{LOG} values are above 0.80 and

309 0.70 respectively. These two goodness-of-fit statistics indicate that GR6J adequately reproduces observed river
310 flow regime, from low to high flow conditions. The less satisfactory performances of GR6J are observed for the
311 Tarn and Roizonne River basins, both characterized by smallest drainage areas and highest elevations of the
312 dataset. These lowest performances are likely to be linked to their location in mountainous areas (snowmelt
313 processes are difficult to reproduce) and to their size (the grid resolution of the baseline climatology fails to capture
314 the climate variability in the headwaters).

315 4.3 The water restriction level modelling framework

316 The Water Restriction Level (WRL) modelling framework developed aims to identify periods when the
317 hydrological monitoring indicator is consistent with legally-binding water restrictions. Only physical components
318 (mainly hydrological drought severity) leading to WR decisions are considered, with no socio-political factor
319 accounted for to model water restrictions.

320 To enable comparison of results across all catchments – in particular to combine response surfaces obtained
321 from different catchments (see Section 5.1) - the same drought monitoring indicators and regulatory thresholds
322 were adopted in all the catchments (see Section 3 for details), selected as most commonly used in the 28 DMPs
323 across the RM district, specifically $VC3$ as monitoring indicator and $10d-VCN3$ with return periods T of 2, 5, 10
324 and 20 years as regulatory thresholds. Each regulatory threshold is defined for a 10-day calendar period between
325 1st April and 31st October, resulting in 21 sets of four thresholds. Water restrictions are decided after consulting
326 drought committees that convene irregularly depending on hydrological conditions over a time window, *i.e.*, the
327 last N days. Here a time window for analysis of $N= 10$ days was decided, which is consistent with the prefectural
328 decision-making time frame (frequency of updates in water restriction statements). The WRL modelling time-step
329 is finally fixed to 10 days and a representative value of WRL is given to the 21 10-day calendar periods from April
330 to October. Thus WRL is thus computed as follows:

- 331 - $VC3(t)$ is computed from daily discharge $Q_{daily}(t)$ every day t ;
- 332 - $VC3(t)$ is compared to the corresponding regulatory thresholds to create time series of daily water
333 restriction level wrl , with $wrl(t)$ ranging from 0 ('no alert') to 3 ('crisis'):
 - 334 ○ if $10d-VCN3(2) \geq VC3(t) > 10d-VCN3(5)$, $wrl(t)=0$
 - 335 ○ if $10d-VCN3(5) \geq VC3(t) > 10d-VCN3(10)$, $wrl(t)=1$
 - 336 ○ if $10d-VCN3(10) \geq VC3(t) > 10d-VCN3(20)$, $wrl(t)=2$

- 337 ○ if $10d\text{-}VCN3(20) \geq VC3(t)$, $wrl(t)=3$
- 338 - A $WRL(d)$ time series is created as the median of $wrl(t)$ for each 10-day period;
- 339 - The $WRL(d)$ value is set to zero if preceding 10-day precipitation total exceeds 70% of inter-annual
- 340 precipitation average(precipitation correction).

341 Inputs of the WRL model are daily discharges and precipitation. Outputs are WRL time series with values for each
342 21 10-day calendar period from April to October. Modelling is only applied to the period April-to-October, the
343 irrigation period and when most water restrictions are put in place. The low-flow monitoring indicator $VC3$ and
344 the regulatory thresholds $10d\text{-}VCN3(T)$ are computed from daily discharge time series Q_{daily} based on full period
345 of records prior to 31st December 2013. The log-normal distribution is used to assess the return periods.

346 The WRL modelling framework can be applied to both observed and simulated time series. For the later, outputs
347 from GR6J are used for simulations under current and modified climate conditions. Regulatory thresholds are
348 derived from simulated discharge using the Safran baseline meteorological reanalysis as input, to moderate the
349 possible effect of bias in rainfall-runoff modelling.

350 The WRL modelling framework was verified in the 15 evaluation catchments (Table 1). WRL simulations based
351 on modelled (hereafter “GR6J”) and observed (hereafter ‘HYDRO’) discharge were compared graphically to
352 official WR measures (“OBS”). A further assessment was conducted using the *Sensitivity* and *Specificity* scores
353 (Jolliffe and Stephenson 2003) to examine how well the WRL modelling framework can discriminate WR severity
354 levels (Table 4). The *Sensitivity* score assesses the probability of event detection; the *Specificity* score calculates
355 the proportion of “No” events that are correctly identified. An event was defined as any legally-binding Water
356 Restriction of at least level 1, and ‘non-event’ a period where WRL is 0 or without WR. Comparisons were made
357 over the 2005-2013 period, corresponding to the common period of availability for OBS, HYDRO and GR6J.

358 Fig. 6 shows years with severe simulated WRLs (e.g., 2005 and 2011) and years with no or few simulated WRs
359 (e.g., 2010 and 2013). Both GR6J and HYDRO simulations are generally consistent with OBS, even if misses are
360 found (e.g., basins 9 to 11 during the year 2005). There is no systematic bias, with some overestimations (e.g.,
361 2005 using GR6J in basins 1 and 15; 2007 using HYDRO in basin 15), underestimations (e.g., 2009 in basin 6, 7,
362 and 8) and misses (e.g., 2005 using HYDRO in basin 1).

363 *Sensitivity* and *Specificity* scores computed with OBS considered as benchmark (Fig. 7) show a large variation
364 across the catchments, in particular for *Sensitivity*. *Specificity* scores are around 0.85 for both GR6J and HYDRO,

365 suggesting that more than 85% of the observed non-events were correctly simulated by the WRL modelling
366 framework. The median of WRL *Sensitivity* score with HYDRO is around 45%, indicating that for half the
367 catchments, less than 45% of observed events are detected based on HYDRO discharges, but this raises to 68% of
368 events detected when WRLs are simulated based on GR6J discharge. Using GR6J is more effective for detecting
369 legally-binding restriction than using observed discharges while it is less efficient for predicting periods without
370 restriction for most of the catchments. There is a compensatory effect, which is not easy to detect graphically since
371 *Sensitivity* scores are more sensitive than *Specificity* scores due to the reduced number of observed days with
372 adopted restrictions. No evidence of systematic bias associated with catchment location or river flow regime was
373 found: northern (blue) and southern (red) catchments are uniformly distributed in the *Sensitivity/Specificity* space.

374 *Sensitivity* and *Specificity* scores using HYDRO as benchmark in the contingency table were also used to
375 compare simulations from GR6J discharge with those obtained from HYDRO discharge. Median values reach
376 84% (*Sensitivity*) and 92% (*Specificity*), showing high consistency between HYDRO and GR6J. No statistical link
377 between hydrological model and WRL model performance was found, with R^2 between NSE_{LOG} and *Sensitivity*,
378 or NSE_{LOG} and *Specificity* lower than 7%. In addition, the similar skill scores of GR6J and HYDRO modelling
379 suggest that possible biases in rainfall-runoff modelling does not impact on the ability of the WRL modelling
380 framework to correctly simulate declared or not declared WRs.

381 Choosing the same definitions for the monitoring indicator and regulatory thresholds is a simplifying assumption
382 and may partly explain the deviations between simulated (HYDRO or GR6J) and adopted (HYDRO) WR
383 measures. Before stating for VC3 and 10d-VCN3 the four prevalent modalities found in the current DMPs have
384 been tested to reproduce observed WR and results has shown a weak sensitivity to the hydrological variables
385 considered in the WR modelling framework. The mains reasons are that all the indicators and thresholds are
386 derived from *Qdaily* time series, are highly correlated and thus share, above all, the same information on the
387 dynamics and on the severity of drought.

388 Heterogeneity in basin characteristics and rules imposed by the DMPs should not result in a systematic difference
389 in *Sensitivity* and *Specificity* score between GR6J and HYDRO identified for most of the 15 evaluation catchments.
390 Simulations were made on near pristine catchments and thus water uses are unlikely to be the main reason. Other
391 causes of higher *Sensitivity* scores obtained when simulated discharges are used as input have been investigated in
392 the WRL modeling framework. However, results of this analysis have not been conclusive. The aforementioned
393 tests with the four prevalent modalities have all led to higher *Sensitivity* score using GR6J and higher *Specificity*

394 score using HYDRO, demonstrating that the choice of the monitoring indicator and regulatory thresholds is
395 probably not involved. A “smoothing” introduced by the hydrological modelling was also suspected but
396 autocorrelation in observed and GR6J simulated VC3 time series was found very similar. Future works may re-
397 investigate these aspects. They will need to explore new ones (e.g., the way WRL is derived from the daily values
398 *wrl* for each 10-day period) using a longer verification period with not necessary uniform but fixed regulatory
399 framework. Indeed some catchments have experienced only three years with legally-binding water restrictions and
400 DMP have been frequently during the 2005-2013 period (see the black vertical segments in Fig. 6).

401 Discrepancy between simulated and adopted WR measures is most likely due to the other factors involved in the
402 making-decision process. When regulatory thresholds are crossed, restrictive measures should follow the DMPs.
403 In reality, the measures are not automatically imposed, but are the result of a negotiating process. This process
404 includes for example some expert-judgment factors such as (i) the evolution of low-flow monitoring indicators
405 and thresholds over the years (e.g., annual revision for the Ouche, and irregular revision for the Isère (38), Gard
406 (30), Alpes-de-Haute-Provence (04) and Lozère (48) departments (last one in 2012)); (ii) the role of drought
407 committees in negotiating a delay in WR level applications to limit economic damages or to harmonize responses
408 across different administrative sectors sharing the same water intake; (iii) the local expertise especially regarding
409 the uncertainty in flow measurements (Barbier *et al.* 2007) impacting on the low-flow monitoring indicators, e.g.,
410 Cote d’Or (21) and Lozère (48) in the northern and southwestern parts of the RM district, respectively. Note that
411 where WR decisions are not uniquely based on hydrological indicators but also involve a negotiation process, the
412 results of the WRL modelling framework should be interpreted as potential hydrological conditions for stating
413 water restrictions.

414 Results of our sample study on 15 evaluation catchments show deviations for most catchments, but links between
415 order restrictions and hydrological drought severity. These deviations may partly be attributed to the use of the
416 same monitoring indicator and regulatory thresholds across the catchments in the modelling (whilst it is not true
417 in reality), as a necessary assumption for a region scale analysis. Tests with *QC7* as low-flow monitoring variable
418 combined with the two dominant modalities for the regulatory thresholds show a weak sensitivity of the WRL
419 modelling skill to the choice of the indicators (with a slight increase in *Specificity* score (~ 90%) while *Sensitivity*
420 score is reduced (< 50%) using GR6J). Whilst the developed WRL modelling framework does not account for
421 expert-decision brought by drought committees - and hence is not designed to simulate the exact WR decisions -
422 its ability to simulate 68% of the stated restrictions over the period 2005-2013 demonstrates its usefulness as a tool

423 to objectively simulate the potential of drought restrictions based on hydrological drought physical processes. The
 424 methodology was applied to the 106 catchments of the RM district under climate perturbations to assess the
 425 potential impact of climate change on water restriction in the region. The resulting analysis focuses on water
 426 restriction level higher than 1, denoted thereafter WR*.

427 **4.4 The generation of perturbed climate conditions**

428 The generation of climate response surfaces relies on synthetic climate time series representative of each explore
 429 climate condition, and used as input to the impact modelling chain (here hydrological model and WRL modelling
 430 framework). Methods based on stochastic weather simulation have been used (Steinschneider and Brown 2013,
 431 Cipriani *et al.* 2014, Guo *et al.* 2016, 2017), but they can be complex to apply in a region with such heterogeneous
 432 climate as the RM district. Alternatively, the simple “delta-change” method (Arnell 2003) has been commonly
 433 used to provide a set of perturbed climates in scenario-neutral approach (Paton *et al.* 2013, Singh *et al.* 2014), and
 434 was used here, similarly to (Prudhomme *et al.* 2010, 2013a, 2013b, 2015).

435 Following Prudhomme *et al.* (2015), monthly correction factors ΔP and ΔT are calculated using single-phase
 436 harmonic functions:

$$437 \quad \Delta P(i) = P_0 + A_p \cdot \cos \left[(i - \varphi_p) \cdot \frac{\pi}{6} \right]. \quad (1)$$

$$438 \quad \Delta T(i) = T_0 + A_T \cdot \cos \left[(i - \varphi_T) \cdot \frac{\pi}{6} \right]. \quad (2)$$

439 with P_0 and $T_0 + A_T$ mean annual changes in precipitation (1) and temperature (2), respectively; i indicator of the
 440 month (from 1 to 12); φ_p the phase parameter and A_p the semi-amplitude of change (e.g., half the difference
 441 between highest and lowest values). These corrections factors were applied to the baseline climate data sets to
 442 create perturbed daily forcings:

$$443 \quad P^*(d) = P(d) \cdot [\overline{PM}(\text{month}(d)) + \Delta P(\text{month}(d))] / \overline{PM}(\text{month}(d)) \quad (3)$$

$$444 \quad T^*(d) = T(d) + \Delta T(\text{month}(d)) \quad (4)$$

445 with $P(d)$ and $T(d)$ baseline precipitation and temperature values for day d ; $P^*(d)$ and $T^*(d)$ the corrected (or
 446 perturbed) values for day d ; $\overline{PM}(\text{month}(d))$ average monthly baseline precipitation for $\text{month}(d)$. Corrected
 447 potential evapotranspiration PET^* time series were derived from temperature values using the formula suggested
 448 by Oudin *et al.* (2005):

449
$$PET^*(d) = \max \left[PET(d) + \frac{Ra}{28.5} \frac{\Delta T(\text{month}(d))}{100}; 0 \right] \quad (5)$$

450 with $PET(d)$ baseline potential evapotranspiration values for day d ; Ra extra-terrestrial global radiation for the
 451 catchment.

452 The baseline climate (precipitation and temperature) time series were extracted from the Safran reanalysis over
 453 the period 1958-2013 (56 years), and perturbed time series generated for the same length. The range of climate
 454 change factors to generate the perturbed series were chosen to encompass both the range and the seasonality of
 455 RCM-based changes on projections in France. A set of 45 precipitation and 30 temperature scenarios was created
 456 (Fig. 8), spanning the range of potential future climate suggested by Terray and Boé (2013) and combined
 457 independently, resulting in a total of 1350 precipitation and temperature perturbations pairs used to define the
 458 climate sensitivity space. In this application,

- 459 - P_0 (mm.an⁻¹) = $-20 + 20/3 \times (j-1)$, $j= 1, \dots, 9$,
- 460 - A_p (mm.season⁻¹) = $20/3 \times (j-1)$, $j= 1, \dots, 5$,
- 461 - T_0 (°C.an⁻¹) = $j-1$, $j= 1, \dots, 6$,
- 462 - A_T (°C.season⁻¹) = $-0.5 + 2 \times (j-1)$, $j= 1, \dots, 5$,
- 463 - φ_P parameter is fixed to 1 to consider minimum change in January and maximum change in July and
- 464 - φ_T is fixed to 2 to get maximum change in August.

465 **4.5 The assumptions on water uses**

466 Water uses and the feedbacks between use and available resources are not explicitly addressed in this application,
 467 either under current or future conditions. This should not be considered as a limitation for basins where
 468 hydrological modelling has been implemented. Indeed, the 106 basins under study have been carefully chosen
 469 since they are currently little or not influenced by human actions. These catchments are benchmark catchments
 470 where natural water availability is monitored for the statement of restriction orders. Water can be abstracted from
 471 other neighboring rivers. Water needs will probably evolve in the next decades. Water requirement for irrigation
 472 may increase in parallel to air temperature or may decrease due to adaptive actions (e.g. farmers may choose to
 473 plant specific crops less sensitive to water shortages). Water needs and sensitivity to water restrictions depend on
 474 socio-economic and institutional pathways. Forward-looking studies have been recently carried out with the
 475 involvement of local experts but at the local scale (Grouillet *et al.* (2015) for the Hérault River basin; Andrews
 476 and Sauquet (2016) for the Durance River basin). The distinct underlying assumptions make difficult to combine

477 and to extend the prospective scenarios over the RM district. Thus, the water restriction modelling framework
478 considers, in this application, the “Business-as-usual” scenario, which assumes that only minor change in water
479 demand behavior will occur. In particular, no major alteration of the river flow regime is projected for the 106
480 catchments. Despite unrealistic, maintaining the current conditions allows assessing the impact of climate change
481 regardless of any other human-induced changes. The advantage is that results are easier to understand and to
482 embrace by stakeholders than those obtained with complex multi-sectorial scenarios they may not identify with.

483 **5 Drought management plans under climate change and their impact on irrigation use**

484 **5.1 The Water Restriction response surfaces**

485 The 1350 sets of perturbed precipitation, temperature and PET time series were each fed into the WRL modelling
486 framework for each 106 catchments. Both $VC3$ (monitoring indicators) and $10d-VCN3(T)$ (regulatory thresholds)
487 were computed from GR6J 56 years discharge simulations. For each scenario, the number of 10-day periods under
488 Water Restriction of at least level 1 (WR^*) were calculated, and expressed as deviation from the simulated baseline
489 value: ΔWR^* , hence removing the effect of any systematic bias from the WRL modelling framework. Results are
490 shown as WR response surfaces built with x - and y -axes representing key climate drivers. Because different climate
491 perturbation combinations share the same values of the key climate drivers, hence represented at the same location
492 of the response surface, the median ΔWR^* from all relevant combinations is displayed as color gradient, with the
493 standard deviation Sd of ΔWR^* showed as size of the symbol.

494 Response surfaces based on different climate variables for x (precipitation) and y (temperature) were generated
495 over full or part of the water restriction period (April to October “AMJJASO”, March to June “MAMJ”; and July
496 to October “JASO”, the latter coinciding with the highest temperatures) and visually inspected to identify the
497 greatest signal pattern, combined with the smallest dispersion around the surface response (*i.e.*, analysis of the
498 median and the maximum of Sd values over the grid cells).

499 The response surfaces are exemplified on three of the 15 evaluation catchments (Table 1, Fig. 9):

- 500 - The Argens River basin, along the Mediterranean coast, severe low-flows occur in summer and actual
501 evapotranspiration is limited by water availability in the soil,
- 502 - The Ouche River basin, in the northern part of the RM district, has a typical pluvial river flow regime under
503 oceanic climate influences, where runoff generation is less bounded by evapotranspiration processes,

504 - The Roizonne River basin, in the Alps, typical of summer flow regime controlled by snowmelt, with spring
505 to summer climate conditions dominating changes in low-flows.

506 The visual inspection of response surfaces shows that:

507 - ΔWR^* are differently driven by the changes in precipitation ΔP and in temperature ΔT : ΔWR^* is very
508 sensitive to ΔP in the Argens River basin (horizontal stratification in the response surface) and to ΔT in the
509 Roizonne River basin (vertical stratification in the response surface) whilst being controlled by both drivers
510 in the Ouche River basin;

511 - There is a high likelihood of increase in the duration of water restriction in the Roizonne River basin, as
512 showed a response surface dominated by positive ΔWR^* ;

513 - Sd values may vary significantly from one graph to another (Table 5). For both the Argens and Roizonne
514 River basins, largest Sd are found when the response surfaces are displayed with climate variables computed
515 over the whole period April-to-October (AMJJASO) while smallest Sd are associated with ΔP and ΔT
516 drivers from March to June. Changes in mean spring to early summer precipitation and temperature mainly
517 govern changes in WR^* for these two basins. Conversely changes in precipitation ΔP and temperature ΔT
518 over the full period April-to-October seem the dominant drivers of changes in WR^* for the Ouche River
519 basin.

520 **5.2 Response surface analysis at the regional scale**

521 Following (Köplin *et al.* 2012, Prudhomme *et al.* 2013a), the 106 response surfaces were classified to define
522 typical response surfaces, designed as tools to help prioritizing actions for adapting water management rules to
523 future climate conditions in the RM district. Here a hierarchical clustering based on Ward's minimum variance
524 method and Euclidian distance as similarity criteria (Ward 1963) was applied and four classes were identified after
525 inspection of the agglomeration schedule and silhouette plots (Rousseeuw 1987). A manual reclassification was
526 conducted for the few catchments with negative individual silhouette coefficients to ensure higher intra-class
527 homogeneity. For each class, a mean response surface and associated Sd was computed, and main climate drivers
528 associated with WR changes identified (Table 5).

529 All suggest an increase in the occurrence of legally-binding water restrictions when precipitation decreases or
530 when temperature increases (Fig. 10). Additional temperature increase and its associated PET increase can

531 compensate for precipitation increase and lead to decrease in ΔWR^* with intra-class differences emerging in the
532 magnitude of changes. The identified four typical Water Restriction response surfaces show a weak regional
533 pattern and common features. Class 4 (including the Roizonne River basin) regroups snowmelt-fed river flow
534 regimes in the Alps, whilst basins of Class 1 are mainly Mediterranean river flow regimes. Class 2 (including the
535 Ouche River basin) and Class 3 catchments are partly influenced by both precipitation and temperature, with
536 ΔWR^* in Class 2 catchments less sensitive to climatic changes (flatter WR response surface) than catchments of
537 Class 3. Flow regime of Classes 2 to 3 ranges from rainfall-fed regimes with high flow in winter and low flow in
538 summer in the northern part of the RM district to regimes partly influenced by snowmelt with high-flows in spring
539 in the Alps and in the Cevennes.

540 To further the regional analysis and help sensitivity assessment at un-modelled catchments, basin descriptors
541 were investigated as possible discriminators of the four classes. A set of potential discriminators - which included
542 measures of the severity, frequency, duration, timing and rate of change in low-flow events (Table 6), the drainage
543 area and the median elevation for the catchment and one climate descriptor (mean annual precipitation and mean
544 annual potential evapotranspiration used to compute an aridity index) – were introduced in a CART model
545 (Classification And Regression Trees, Breiman *et al.* 1984), aimed at performing successive binary splits of a
546 given data set according to decision variables. Through a set of “*if-then*” logical conditions the algorithm
547 automatically identifies the best possible predictors of group membership, starting from the most discriminating
548 decision variable to the less important factors. The optimal choices are fixed recursively by increasing the
549 homogeneity within the two resulting clusters. At each step one of the clusters (node) is divided into two non-
550 overlapping parts. Here, to free results from catchment size influence, descriptors related to severity were
551 expressed in mm/year, mm/month or mm/day.

552 Results show three top discriminators, the aridity index being the strongest:

- 553 - Aridity index *AI* given by the mean annual precipitation divided by the mean annual potential
554 evapotranspiration (UNEP, 1993),
- 555 - Baseflow index *BFI*, a measure of the proportion of the baseflow component to the total river flow, calculated
556 by the separation algorithm separation suggested by Lyne and Hollick (1979),
- 557 - Concavity Index *IC* (Sauquet and Catalogne 2011) to characterize the contrast between low-flow and high-
558 flow regimes derived from quantiles of the flow duration curve,

559 CART overall misclassification (18%) suggests a satisfactory performance in classification method,
560 characterized by a parsimonious algorithm (five nodes and three variables) with potential for a first guess
561 assessment of the WR response to disruptions and evaluation of the robustness of existing water restriction at the
562 department-level scale. For each class, Fig. 11 shows the empirical distribution of the three main discriminators,
563 the mean timing θ of daily discharge below Q_{95} and its dispersion r , based on circular statistics, where Q_{95} is the
564 95th quantile derived from the flow duration curve.

565 The classification discriminates catchments primarily on the seasonality of low-flow conditions and the aridity
566 index, with the extreme classes (1 and 4) being particularly well discriminated.

567 Geographically, Class 1 catchments are mainly located along the Mediterranean coast and include the Argens
568 River basin; ΔWR^* is mainly driven by changes in precipitation in spring and early summer. Class 1 gathers water-
569 limited basins with small values of AI and a weak sensitivity to climate change in summer. In these dry water-
570 limited basins, the mid-year period exhibits the minimal ratio P/PET and changes in summer precipitation has
571 hence only a moderate impact on low-flows; spring is the only season when PET changes are likely to result in
572 both actual evapotranspiration and discharge changes. WR levels are more likely controlled by antecedent soil
573 moisture conditions in spring and early summer. This behavior is typical of the basins under Mediterranean
574 conditions and was discussed in the context of a scenario-neutral study in Australia (Guo *et al.* 2016). For those
575 catchments, climate drivers computed in spring (over the period MAMJ) are used to describe the x- and y-axes of
576 the response surface, fully consistent with water-limited basin processes.

577 Catchments of both Class 2 and 3 have similar IC , hence suggesting that flow variability is not a proxy for low-
578 flow response to climatic deviation. However, BFI values for Class 3 are lower than for Class 2 while Class 3 is
579 characterized by high values for AI . Despite higher capability to sustain low-flows (see BFI values) the response
580 surface representative of Class 2 is more contrasted than that of Class 3; a possible reason could be drier conditions
581 under current conditions (the median of AI equals 2.5 for Class 3 against 1.6 for Class 2). The monthly perturbation
582 factors (see Sect. 5.1) are the same for all the classes but the changes in relative terms are less significant regarding
583 the current climate conditions for Class 3 than for Class 2, and may explain the limited changes in river flow
584 patterns.

585 Class 4 regroups catchments with low flows in winter and significant snow storage. The BFI values are high and
586 due to smooth flow duration curves, IC demonstrates also high values.

587 5.3 Risk assessment at the basin scale

588 The risk-based framework has been applied to the irrigation water use since annual net total water withdrawal
589 for agriculture purposes is ranked first at the regional scale. Note that in the Rhône-Méditerranée district around
590 90% and 10% of water used for irrigation originate from surface water and groundwater, respectively. To
591 complement water needs irrigators may also have access to small reservoirs (storage capacity usually less than 1
592 Mm³). Most of the reservoirs are filled by surface water in winter and release water later in the following summer.
593 Water restrictions are not imposed to these reservoirs but it is assumed here that during severe drought events the
594 majority of them are empty and thus the existence of potential sources auxiliary to surface water on the conclusions
595 has limited influence on the conclusions.

596 We assumed here that irrigated farming is globally under failure if the duration with limited or suspended
597 abstraction is above a critical threshold T_c that causes insufficient water for crops. The catchment or area i will be
598 considered more vulnerable than the catchment or area j if the likelihood of failure (*i.e.*, exceeding T_c) for
599 catchment or area i is more than the likelihood of failure for catchment or area j . The critical threshold T_c is a value
600 of total number of days with legally-binding water restrictions that needs to be fixed. To move closer to reality and
601 following Simonovic (2010), the value of T_c is based on the analysis of past events. A possible way to fix T_c is to
602 simulate historic drought events observed during the period 2005-2012 and the effects of water restrictions on crop
603 yield and quality and on economic losses. Computing water deficits was considered rather tricky at the farming
604 scale - partly due to the high heterogeneity in crop and soil types, watering systems, conveyance efficiencies, etc.
605 across the RM district - and we have investigated the use of ‘agricultural disaster’ notifications as proxies to
606 identify the damaging conditions instead.

607 Specifically the ‘agricultural disaster’ notifications are issued by the agriculture ministry following
608 recommendations from the Prefecture to each department affected by extreme hydro-meteorological events, and
609 applied uniformly over the RM district. Whilst ‘agricultural disaster’ status is a global index that may mask
610 heterogeneity in crop losses within each department, and that reflects losses related to both agricultural and
611 hydrological droughts, it has the advantage of being directly related to economic impact, and uniformly applied
612 across the RM district, hence suitable for a regional-scale analysis. The national system of compensation to farmers
613 is initiated for areas notified under ‘agricultural disaster’ status.

614 Over 2005-2012, only one agriculture disaster was declared, in 2011, and applied to 70 of the 95 departments in
615 continental France, and to 16 of the 28 departments fully or partly located in the RM district. Data are collected
616 by the French Ministry of Agriculture and Food and they are not publically available. The year 2011 was the only
617 year when the national system of compensation has been triggered between 1958 and 2013 and the analysis of
618 simulated water restrictions for this year fixed the value for T_c . The duration of water restrictions was calculated
619 individually for each catchment and converted into anomalies $\Delta WR^*(2011)$ with respect to the benchmark value
620 (mean over the period 1958-2013). For consistency with the indicators used in the response surfaces, this threshold
621 $\Delta WR^*(2011)$ is derived from GR6J outputs.

622 The RCM-based projections of all the catchments of the class for the three time slices 2021-2050, 2041-2070
623 and 2071-2100 were superimposed to the representative response surfaces to assess the risk of failure (Fig. 4).
624 Finally the vulnerability resulting from the combination of the three components sensitivity, performance and
625 exposure was measured by the proportion of RCM-based projections leading to critical situations, similarly to
626 Prudhomme *et al.* (2015). Technically this Vulnerability Index (VI) calculated as the proportion of exposure
627 simulations that fail below the critical threshold T_c is the complement to the “climate-informed” robustness index
628 (CRI) (Whateley *et al.* 2014). Given one specific climate projection, a catchment or a group of catchments could
629 be judged vulnerable if on average T_c is exceeded. VI is introduced here to account for the uncertainty in climate
630 projections in risk assessment. This index should be interpreted as conditional probability (risk) with respect to a
631 specified ensemble of future climates.

632 Fig. 12 shows an application to the Ouche River basin, North of the RM district (1, Fig. 1, Table 1) and declared
633 under agricultural disaster status in 2011. The black dotted line are isopleths connecting points of the response
634 surface with $\Delta WR^* = \Delta WR^*(2011) = T_c$ (= 7 10-day periods for this catchment), and delimits the climate space
635 leading to median climatic situations more severe than 2011 ($\Delta WR^* > \Delta WR^*(2011)$, above left) or less severe than
636 2011 ($\Delta WR^* < \Delta WR^*(2011)$, below right) $\Delta WR^*(2011)$. As reference, the black solid line ($\Delta WR^* = 0$) delimits
637 the climate space associated with more (above left) or less (bottom right) water restrictions compared with the
638 whole period average (1958-2013). Basin-scale exposure projections (Table 2) were plotted onto the WR response
639 surface for three time-slices 2021-2050, 2041-2070 and 2071-2100 (grey symbols), showing a warmer trend but
640 no total precipitation signal. Whilst by the end of the century, projections move towards the critical threshold
641 $\Delta WR^*(2011)$ climate space, pointing out a significant increase in more severe low-flows, there remain a large
642 spread in signal (dispersion of the grey symbols) and the vulnerability index equals zero for this catchment.

643 5.4 A regional perspective for prioritizing adaptation strategies

644 Following the methodology applied to the Ouche River basin, $\Delta WR^*(2011)$ were calculated for individual
645 catchments and averaged to produce a value of T_c relevant for each Class (Table 7). Class variation in $\Delta WR^*(2011)$
646 is large, with Class 2 and 3 showing thresholds of at least 7 10-day periods, whilst they are close to zero for Class
647 1 and Class 4. The scatter in the $\Delta WR^*(2011)$ values is certainly due to heterogeneity in crops, in irrigation
648 systems, in climate conditions, etc. at the regional scale leading to locally differentiated sensitivity to water
649 restrictions as well as to biases in WR modelling. Since only the year 2011 it is now difficult to conclude on the
650 origins of the dispersion (natural or non-natural). However the distribution and absolute values of the critical
651 thresholds reflect well the spatial pattern of WR enforced from May to September 2011, with Southern regions
652 and the French Alps moderately affected by lack of rainfall in spring compared to the Northern and Western
653 regions of the RM district (Fig. 13). Surprisingly negative values for $\Delta WR^*(2011)$ are found for some catchments
654 of Classes 1 and 4, providing no evidence to support their agricultural disaster status that year. At the RM scale,
655 average $\Delta WR^*(2011)$ equals 38 days when considering all catchments, and increases to 66 days when considering
656 only catchments under agricultural disaster status. Simplifying but realistic assumptions are imposed by the lack
657 of detail information; thus only one value was considered at the regional scale despite high dispersion in
658 $\Delta WR^*(2011)$ values (Table 7): the critical threshold T_c was set to the average of the $\Delta WR^*(2011)$ values computed
659 on all catchments in departments under agricultural disaster status in 2011 (6.6 10-day periods), and was used
660 thereafter for all classes. Note that this value of T_c seems realistic: it represents a significant period with restrictions
661 (66 days or 30% of the time between the 1st April and the 31st October).

662 Using the Class WR response surface as diagnostic tools, exposure information (grey symbols) and thresholds
663 ($\Delta WR^*=0$, solid, $\Delta WR^*(2011)$, dashed black lines) were displayed (Fig. 14), and VI calculated (Table 7). The
664 location of the two isopleths $\Delta WR^* = \Delta WR^*(2011)$ (black dotted line) and $\Delta WR^* = 0$ (black straight line) in the
665 WR response surface depends on the shape of the response surface and differ from one class to another. The portion
666 of the WR response surface associated with $\Delta WR^* < 0$ is gradually lower from Class 1 to Class 4 suggesting that
667 catchments of Class 4 are more subject to an increase in water restriction occurrence than catchments of the other
668 classes. Classes 1 and 4, the most extreme responses classes, contain fewer catchments, whilst Classes 2 and 3,
669 characterized by an intermediate response, have the most of the catchments. Because of the large geographical
670 spread of catchments of Class 2 and 3, an expert-based division was done to distinguish catchments with
671 continental (northern sectors) and Mediterranean (southern sectors) climate in terms of exposure. This is to better

672 capture the predominantly north–south gradient in future projections of both temperature and rainfall, as they
673 differing impact on the river flow regime (e.g., Boé *et al.* 2009; Chauveau *et al.* 2013; Dayon *et al.* 2018). For all
674 classes, vulnerability increases with lead time, with Class 4 showing the largest vulnerability and Class 1 being
675 the less vulnerable despite its location in the Mediterranean area. In the two classes 2 and 3, vulnerability increases
676 from North to South in the RM district ($VI = 13\%$ for Class 2-N against 32.9% for Class 2-S at the end of the
677 century). These contrasted results are mainly explained by the difference between exposure characterizations since
678 a common value of the threshold T_c was adopted.

679 **5.4 Water restriction policy implementation**

680 In 2011, France adopted a general framework for action—the French National Climate Change Impact
681 Adaptation Plan (“Plan National d’Adaptation au Changement Climatique (PNACC)” in French)—with numerous
682 recommendations related to research and observation. Five priorities of the first PNACC related to water resources
683 have been highlighted. The PNACC has been recently reviewed and the PNACC2 published in December 2018
684 confirms the place of DMPs as tools for monitoring water resources and water allocation, and for driving greater
685 public and stakeholder awareness ([https://www.ecologique-solidaire.gouv.fr/adaptation-france-au-changement-](https://www.ecologique-solidaire.gouv.fr/adaptation-france-au-changement-climatique)
686 [climatique](https://www.ecologique-solidaire.gouv.fr/adaptation-france-au-changement-climatique)).

687 However and until now, impacts of future climate change is not account for in DMPs. The development of DMPs
688 have helped to ease past conflicts at the department scale. Water users are now facing more frequent water
689 restrictions (more than half France have departments experiencing $WR \geq 1$ between 2011 and 2018 (Fig. 15)) and
690 the timing and the level of the restrictions vary from one year to another: the highest number of French departments
691 with $WR \geq 1$ was observed in summer in both 2015 and 2017 while the year 2018 was characterized by late water
692 restrictions (mostly in autumn). Stakeholders are now questioning the DMP implementation, but only at the short
693 term – the impact of climate change is not yet a subject matter. One of their main concerns is the heterogeneity in
694 current restrictions levels and timing from one department to another or from the upstream to the downstream part
695 of the catchment. One of the option being considered to address this challenge in southeastern France is to
696 harmonise the definition of the regulatory thresholds, at the regional scale. Results obtained here show that the
697 standardisation will probably not fix the problem due to the balance between socio-political and hydrological
698 factors in the final WR statement.

699 The map displaying the class membership could be a convenient tool for local authorities to discuss the spatial
700 heterogeneity in terms of impact to drought on water restrictions under both current and future climate conditions.

701 Despite operating rules uniformly applied, there is a high variability in catchments responses within the department
702 (see the southernmost department in Fig. 10). Therefore, any investigation on DMPs at the department level
703 disregarding this heterogeneity will be biased. The sensitivity analysis provides information for local authorities
704 to better understand the differences in catchment responses to observed droughts in areas, which fall within their
705 responsibility. For instance, water management in basins of Class 4 could be more problematic during a year with
706 a severe heat wave while it could be more problematic for a year with a pronounced precipitation deficit for
707 catchments of Class 1. It is likely that the differences in the impact of droughts on WR will persist if stakeholders
708 do not question the assumption of a uniform definition for the hydrological indicators within the department.

709 DMPs have been recognized in the PNACC as relevant water management tools and our findings have also
710 implications for adaptation strategies. We have shown that the climate change effects could be felt more acutely
711 during the irrigation period by an increase in water restriction. Thus, relying on surface water to compensate
712 deficits is highly hazardous. Options under consideration are saving water, enhancing water storage by building
713 new small dams or securing water access by transferring water from the Rhone River (e.g., Ruf 2012), which is
714 considered as an “overabundant” river within the RM district. Saving water is the solution favoured by the RM
715 Water Agency. Creating new storages is increasingly considered as potential solution to secure water for
716 agriculture since they are not subject to water restrictions. Authorising new water storages may also reduce the
717 sense of unfairness among users in areas with no secured access. Most of the small reservoirs are filled by surface
718 water in winter, release water later in summer for irrigation purposes and then limit the pressure on water resource
719 during crises. However, there is actually a wide discussion about these hydraulic structures in France since their
720 cumulative impacts on the ecosystem and their efficiency are not well known (Habets *et al.* 2018). Building
721 adaptation strategies on additional water storage may lead to maladaptation since natural inflows will probably
722 decrease, and delay the mutation of agricultural practices and conservation measures. In addition, there is actually
723 no guarantee that these reservoirs will be filled and that their storage capacity will be enough to cope with severe
724 droughts.

725 The RM Water Agency has taken other the objectives of PNACC at the regional scale and has initiated an
726 unprecedented major initiative that provides guidance for the River Basin Management Plan (2016–2021). The
727 adaptation strategy partly relies on an analysis of the vulnerability in different water-related sectors (water
728 resources, soil-moisture, biodiversity, and water quality) within the RM district to climate change. The study
729 complements this former analysis by focusing here on agricultural uses and meets the requirements for
730 vulnerability assessment carried out by the RM Water Agency: it covers the same area and the methodology is

731 uniformly applied across the area of interest. It may help the RM Water Agency identifying when and where
732 actions and investments are the most needed to mitigate the effects of climate change (probably in catchments of
733 Class 4 from the short perspective, and later for the other areas).

734 **6 Conclusions**

735 This paper presents a first attempt to analyse and simulate water restrictions over a large area in France applying
736 an alternative approach to the classical “top-down” approach. The risk-based approach developed here relies on
737 sensitivity-based analyses to a wide range of climate changes, making it scenario-neutral. However ex ante climate
738 projections are introduced in the last stage of the framework to assess the likelihood of failure.

739 The analysis of the past and current DMPs in the RM district shows a decision-making processes highly
740 heterogeneous in terms of both low-flow monitoring variable and regulatory thresholds. In reality, the WR
741 statements follow a set of rules defined in the DMPs (which can be simulated and reproduced automatically) but
742 also expert judgment or lobbying from key stakeholders - which are not accounted for in the WRL modelling
743 framework put in place here. However, the post-processing of GR6J outputs allows detecting more than 68% of
744 severe alerts (more severe than level 1), making the developed framework a useful tool. Our study is a first step
745 towards a comprehensive accounting of physical processes, but does not capture socio-economic factors, also
746 critically important and reaches out to interdisciplinary for completing the modelling framework designed here.
747 The study at the regional scale illustrates an expected difficulty to simulate accurately a regulatory framework.
748 Further improvement is not expected in enhancing hydrological models but in reproducing decision-making
749 processes. The overall performance could be improved by scrutinizing the minutes of the drought committees to
750 better understand the weight of the stakeholders in the final statement.

751 The sensitivity analysis and the related response surfaces suggest that basins located in the Southern Alps are
752 the most responsive basins to climate change and that those experiencing a high ratio P/PET are found the less
753 responsive. The classification method CART has been applied to 106 responses surfaces associated with 106
754 gauged basins and leads to four classes with different sensitivity. The key-variables known at un-modelled but
755 gauged catchments can be introduced in the decision-tree to finally predict the assignment as a first guess to one
756 of the four classes. Water managers are thus encouraged to monitor in priority and more accurately temperature
757 and/or precipitation when and where the sensitivity of their catchments is found the highest. This may mean efforts
758 to reinforce field instrumentation within these key catchments.

759 Although incomplete, the proposed framework demonstrates, as expected (see Assessment Box SPM.2 Table 1
760 in (IPCC 2014)), a sensitivity of the DMPs to climate changes. The impact of climate change on the river flow is
761 expected to be gradual, thus offering opportunities to update, to harmonize and to adapt Drought Management
762 Plans to changes in climate conditions and water needs. As a consequence, the need for adaptation of existing
763 drought action plans could differ much from one catchment to another and should take into account intrinsic
764 sensitivity to climate change besides ‘top-down’ projections. Results also show needs to firstly adapt DMPs in
765 temperature sensitive catchments more subject to a significant increase in legally-binding restrictions in the short
766 term. In contrast, the capacity to anticipate changes in both the occurrence and severity of WR, and their
767 consequences for water management will be challenging in catchments where water restrictions are mainly driven
768 by precipitation due to their high uncertainties in future regional climate projections.

769 The risk-based approach was applied to assess the vulnerability of irrigation due to regulatory instruments under
770 modified climate. Evaluating the impact of climate change on irrigation was not the objective of the suggested
771 framework; it has been applied to estimate the likelihood of failure for irrigation at various lead times, instead.
772 Usually, a failure can be stated when irrigation water needs are not fully satisfied. This case study suggests the use
773 of a proxy obtained from a national system of compensation to define a critical threshold (maximum acceptable
774 duration with water restriction). Analysis, however, was based on limited data (one year) and a better failure
775 assessment is required using other years (e.g., 2015 and 2017). The higher the probability, the more vulnerable the
776 irrigation use within the department. Finally, socio-economic system stressors like agricultural practices,
777 population growth, water demand, etc. should be considered to highlight combinations that would lead to
778 unacceptable conditions and to assess the performance of various adaptation strategies under an extended set of
779 future climate conditions (Poff *et al.* 2016).

780 Climate response surface appears as a convenient tool for simulating and discussing future perspectives locally
781 on the basin scale or more broadly on a given management territory. For example, they can support implement
782 adaptive strategies (see - as an example - the Robust Decision Making framework suggested by Lempert and
783 Groves (2010)): response surfaces can be drawn for different adaptation scenarios combined with periodic updates
784 of DMPs including rules for defining regulatory thresholds and monitoring variables evolving over time, etc.

785 Note that all results are based on a single hydrological model, but a multi-model approach could be applied as
786 the magnitude of the rainfall-runoff response was shown vary with different hydrological models (e.g., Vidal *et*

787 *al.* 2016; Kay *et al.* 2014). Finally, an extension of the area of interest to the whole France may bring to light a
788 more complete typology of response surfaces and a wider range of sensitivity.

789 **Acknowledgments**

790 The authors thank Météo-France for providing access to the Safran database. Regional projections were obtained
791 from the DRIAS portal (<http://drias-climat.fr/>) and consulted on November 2016. Analyses were performed in R
792 (R Core Team 2016) with packages airGR (Coron *et al.* 2017), chron (James and Hornik 2017), circular (Lund *et*
793 *al.* 2017), doParallel (Calaway *et al.* 2017), dplyr (Wickham and François 2015), ggplot2 (Wickham 2009),
794 hydroTSM (Zambrano-Bigiarini 2014), RColorBrewer (Neuwirth 2014), reshape2 (Wickham 2007), rpart
795 (Therneau *et al.* 2018), scales (Wickham 2016), stringr (Wickham 2017) and zoo (Zeileis and Grothendieck 2005).
796 The study was funded by Irstea and the French RM Water Agency.

797 **References**

- 798 Andrew J.T. and Sauquet E.: Climate Change Impacts and Water Management Adaptation in Two Mediterranean-
799 Climate Watersheds: Learning from the Durance and Sacramento Rivers. *Water* 2017, 9, 126, doi:
800 10.3390/w9020126, 2017.
- 801 Arnell N.W.: Relative effects of multi-decadal climatic variability and changes in the mean and variability of
802 climate due to global warming: future streamflow in Britain. *J. Hydrol.* 270, 19–213, 2003.
- 803 Barbier R., Barreteau O., and Breton C.: Management of water scarcity: between negotiated implementation of the
804 “décret sécheresse” and emergence of local agreements. *Ingénieries - EAT IRSTEA édition 2007*, 3-19, 2007.
- 805 Bisselink B., Bernhard J., Gelati E., Adamovic M., Guenther S., Mentaschi L. and De Roo A.: Impact of a changing
806 climate, land use, and water usage on Europe’s water resources, EUR 29130 EN, Publications Office of the
807 European Union, Luxembourg, 2018, ISBN 978-92-79-80287-4, doi:10.2760/847068, JRC110927, 2018.
- 808 Boé J., Terray L., Martin E., and Habets F.: Projected changes in components of the hydrological cycle in French
809 river basins during the 21st century. *Water Resour. Res.* 45 (8), W08426, doi:10.1029/2008WR007437, 2009.
- 810 Breiman L., Friedman J.H., Olshen R., and Stone C.J.: *Classification and Regression Trees*, Wadsworth, Belmont,
811 California, 1984.
- 812 Brekke L.D., Maurer E.P., Anderson J.D., Dettinger M.D., Townsley E.S., Harrison A., and Pruitt T.: Assessing
813 reservoir operations risk under climate change. *Water Resour. Res.*, 45, W04411, doi:10.1029/2008WR006941,
814 2009.

815 Broderick C., Murphy C., Wilby R.L., Matthews T., Prudhomme C., and Adamson, M. (2019). Using a Scenario
816 - neutral framework to avoid potential maladaptation to future flood risk. *Water Resources Research*, 55.
817 <https://doi.org/10.1029/2018WR023623>

818 Brown C., Werick W., Leger W., and Fay D.: A decision-analytic approach to managing climate risks: Application
819 to the upper great lakes. *Journal of the American Water Resources Association (JAWRA)* 47, 524–534, 2011.

820 Brown C., Ghile Y., Lavery M., and Li K.: Decision scaling: Linking bottom-up vulnerability analysis with
821 climate projections in the water sector. *Water Resour. Res.* 48, W09537, doi:10.1029/2011WR011212, 2012.

822 Brown C., Wilby R.L.: An alternate approach to assessing climate risks. *Trans. Am. Geophys. Union* 93(41), 401–
823 402, 2012.

824 Bubnová R., Hello G., Bénard P., and Geleyn J.F.: Integration of the Fully Elastic Equations Cast in the Hydrostatic
825 Pressure Terrain-Following Coordinate in the Framework of the ARPEGE/Aladin NWP System. *Monthly Weather*
826 *Review* 123 (2), 515-35, 1995.

827 Caillouet L., Vidal J.-P., Sauquet E., Devers A., and Graff B: Ensemble reconstruction of spatio-temporal extreme
828 low-flow events in France since 1871. *Hydrol. Earth Syst. Sci.* 21, 2923-2951, 2017.

829 Calaway R., Microsoft Corporation, Weston S., and Tenenbaum D.: doParallel: Foreach Parallel Adaptor for the
830 'parallel' Package. R package version 1.0.11, <https://CRAN.R-project.org/package=doParallel>, 2017.

831 Chauveau M., Chazot S., Perrin C., Bourgin P.-Y., Sauquet E., Vidal J.-P., Rouchy N., Martin E., David J., Norotte
832 T., Maugis P., and de Lacaze X: What will be the impacts of climate change on surface hydrology in France by
833 2070? *La Houille Blanche* 4, 5-15, 2013.

834 Cipriani T., Tilmant F., Branger F., Sauquet E., and Datry T. : Impact of climate change on aquatic ecosystems
835 along the Asse river network. In “Hydrology in a Changing World: Environmental and Human Dimensions”
836 (Daniell T., Ed.), *AIHS Publ.* 363, 2014, 463-468, 2014.

837 Collet L., Harrigan S., Prudhomme C., Formetta G., and Beevers L.: Future hot-spots for hydro-hazards in Great
838 Britain: a probabilistic assessment, *Hydrol. Earth Syst. Sci.*, 22, 5387-5401, [https://doi.org/10.5194/hess-22-5387-](https://doi.org/10.5194/hess-22-5387-2018)
839 2018, 2018.

840 Coron L., Thirel G., Delaigue O., Perrin C., and Andréassian V.: airGR: A Suite of Lumped Hydrological Models
841 in an R-Package. *Environmental Modelling and Software* 94, 166-171,
842 <https://doi.org/10.1016/j.envsoft.2017.05.002>, 2017.

843 Culley S., Noble S., Yates A., Timbs M., Westra S., Maier H.R., Giuliani M., and Castelletti A.: A bottom-up
844 approach to identifying the maximum operational adaptive capacity of water resource systems to a changing
845 climate. *Water Resour. Res.* 52, 6751–6768, 2016.

846 Danner A., Mohammad Safeeq G., Grant GE., Wickham C., Tullos D., and Santelmann M.V.: Scenario-Based and
847 Scenario-Neutral Assessment of Climate Change Impacts on Operational Performance of a Multipurpose
848 Reservoir. *Journal of the American Water Resources Association (JAWRA)* 53(6), 1467-1482, 2017.

849 Dayon G., Boé J., Martin E., and Gailhard J.: Impacts of climate change on the hydrological cycle over France and
850 associated uncertainties. *Comptes Rendus Geoscience* 350(4), 141-153, 2018.

851 Fronzek S., Carter T.R., and Räisänen J.: Applying probabilistic projections of climate change with impact models:
852 a case study for sub-arctic palsa mires in Fennoscandia. *Climatic Change* 99, 515–534, 2010.

853 Ghile Y.B., Taner M.Ü., Brown C., and Talbi A.: Bottom-up climate risk assessment of infrastructure investment
854 in the Niger River Basin. *Climatic Change* 122(1–2), 97–110, 2014.

855 Giorgi F.: Climate change hot-spots. *Geophys. Res. Lett.*, 33, L08707, doi:10.1029/2006GL025734, 2006.

856 Grouillet B., Fabre J., Ruelland D., and Dezetter A.: Historical reconstruction and 2050 projections of water
857 demand under anthropogenic and climate changes in two contrasted Mediterranean catchments, *J. Hydrol.*, 522,
858 684–696, 2015.

859 Guo D., Westra S., and Maier H.R.: An inverse approach to perturb historical rainfall data for scenario-neutral
860 climate impact studies. *J. Hydrol.* 556: 877-890, 2016.

861 Guo D., Westra S., and Maier H.R.: Use of a scenario-neutral approach to identify the key hydrometeorological
862 attributes that impact runoff from a natural catchment. *J. Hydrol.* <http://dx.doi.org/10.1016/j.jhydrol.2017.09.021>,
863 2017.

864 Gupta, H. V., Kling, H., Yilmaz, K., and Martinez, G. F.: Decomposition of the mean squared error and NSE
865 performance criteria: Implications for improving hydrological modelling, *J. Hydrol.*, 377, 80–91,
866 <https://doi.org/10.1016/j.jhydrol.2009.08.003>, 2009.

867 Habets F., Molénat J., Carluer N., Douez O., and Leenhardt D.: The cumulative impacts of small reservoirs on
868 hydrology: A review. *Sci. Total. Environ.*, 643, 850-867, <https://doi.org/10.1016/j.scitotenv.2018.06.188>, 2018

869 Hellwig J. and Stahl K.: An assessment of trends and potential future changes in groundwater-baseflow drought
870 based on catchment response times, *Hydrol. Earth Syst. Sci.*, 22, 6209-6224, [https://doi.org/10.5194/hess-22-](https://doi.org/10.5194/hess-22-6209-2018)
871 6209-2018, 2018.

872 Hublart P., Ruelland D., García de Cortázar-Atauri I., Gascoin S., Lhermitte S., and Ibacache A.: Reliability of
873 lumped hydrological modeling in a semi-arid mountainous catchment facing water-use changes. *Hydrol. Earth*
874 *Syst. Sci.* 20, 3691-3717, <https://doi.org/10.5194/hess-20-3691-2016>, 2016.

875 IPCC: Summary for policymakers. In: *Climate Change 2014: Impacts, Adaptation, and Vulnerability. Part A:*
876 *Global and Sectoral Aspects. Contribution of Working Group II to the Fifth Assessment Report of the*
877 *Intergovernmental Panel on Climate Change* [Field, C.B., V.R. Barros, D.J. Dokken, K.J. Mach, M.D.
878 Mastrandrea, T.E. Bilir, M. Chatterjee, K.L. Ebi, Y.O. Estrada, R.C. Genova, B. Girma, E.S. Kissel, A.N. Levy,
879 S. MacCracken, P.R. Mastrandrea, and L.L. White (eds.)]. Cambridge University Press, Cambridge, United
880 Kingdom and New York, NY, USA, pp. 1-32, 2014.

881 Jacob D., Petersen J., Eggert B., Alias A., Christensen O.B., Bouwer L.M., and Braun A.: EURO-CORDEX: New
882 high-resolution climate change projections for European impact research, *Regional environmental change* 14(2),
883 563-78, 2014.

884 Jakeman A.J., Littlewood I.G., Whitehead P.G.: Computation of the instantaneous unit hydrograph and identifiable
885 component flows with application to two small upland catchments. *J. Hydrol.*, 117, 275–300, 1990.

886 James D. and Hornik K.: chron: Chronological Objects which Can Handle Dates and Times. R package version
887 2.3-50, <https://CRAN.R-project.org/package=chron>, 2017.

888 Jiménez Cisneros B.E., Oki T., Arnell N.W., Benito G., Cogley J.G., Döll P., Jiang T., and Mwakalila S.S.:
889 Freshwater resources. In: *Climate Change 2014: Impacts, Adaptation, and Vulnerability. Part A: Global and*
890 *Sectoral Aspects. Contribution of Working Group II to the Fifth Assessment Report of the Intergovernmental Panel*
891 *on Climate Change* [Field, C.B., V.R. Barros, D.J. Dokken, K.J. Mach, M.D. Mastrandrea, T.E. Bilir, M.
892 Chatterjee, K.L. Ebi, Y.O. Estrada, R.C. Genova, B. Girma, E.S. Kissel, A.N. Levy, S. MacCracken, P.R.
893 Mastrandrea, and L.L. White (eds.)]. Cambridge University Press, Cambridge, United Kingdom and New York,
894 NY, USA, 229-269, 2014.

895 Jolliffe I.T. and Stephenson D.B.: *Forecast verification. A practitioner's Guide in Atmospheric Science.* John Wiley
896 & Sons Edition, 2003.

897 Kay A. L., Crooks S. M., and Reynard N. S.: Using response surfaces to estimate impacts of climate change on
898 flood peaks: assessment of uncertainty. *Hydrol. Process.*, 28, 5273–5287, <https://doi.org/10.1002/hyp.10000>,
899 2014.

900 Köplin N., Schädler B., Viviroli D., and Weingartner R.: Relating climate change signals and physiographic
901 catchment properties to clustered hydrological response types. *Hydrol. Earth Syst. Sci.* 16: 2267–2283, 2012.

902 Le Moine N.: Le bassin versant de surface vu par le souterrain: une voie d'amélioration des performances et du
903 réalisme des modèles pluie-débit? Ph.D. thesis. Université Pierre et Marie Curie (Paris), Cemagref (Antony), 324
904 pp, 2008

905 Lémond J., Dandin P., Planton S., Vautard R., Pagé C., Déqué M., Franchistéguy L., Geindre S., Kerdoncuff M.,
906 Li L., Moisselin J.M., Noël T., and Tourre Y.M.: DRIAS: a step toward Climate Services in France. *Adv. Sci. Res.*
907 6: 179-186, 2011.

908 Lempert R.J., and Groves D.G.: Identifying and evaluating robust adaptive policy responses to climate change for
909 water management agencies in the American west. *Technological Forecasting and Social Change* 77(6): 960-974,
910 <https://doi.org/10.1016/j.techfore.2010.04.007>, 2010.

911 Lund U., Agostinelli C., Arai H., Gagliardi A., Garcia Portugues E., Giunchi D., Irisson J.O., Pocernich M., and
912 Rotolo F.: circular: Circular Statistics. R package version 0.4-93, <https://CRAN.R-project.org/package=circular>,
913 2017.

914 Lyne V. and Hollick M.: Stochastic time variable rainfall runoff modeling. In: *Proceedings of the Hydrology and*
915 *Water Resources Symposium Berth, 1979. National Committee on Hydrology and Water Resources of the*
916 *Institution of Engineers, Australia, 89–92, 1979.*

917 Mastrandrea M.D., Heller N.E., Root T.L., and Schneider S.H.: Bridging the gap: linking climate-impacts research
918 with adaptation planning and management. *Climatic Change* 100, 87-101, 2010.

919 MEDDE - Ministère de l'Écologie et du Développement Durable (2004) Plan d'Action Sécheresse.

920 Nash J.E. and Sutcliffe J.V.: River flow forecasting through conceptual models Part I – A discussion of principles.
921 *J. Hydrol.* 10(3), 282–290, 1970.

922 Neuwirth E.: RColorBrewer: ColorBrewer Palettes. R package version 1.1-2, [https://CRAN.R-](https://CRAN.R-project.org/package=RColorBrewer)
923 [project.org/package=RColorBrewer](https://CRAN.R-project.org/package=RColorBrewer), 2014.

924 Oudin L., Hervieu F., Michel C., Perrin C., Andréassian V., Anctil F., and Loumagne C.: Which potential
925 evapotranspiration input for a lumped rainfall–runoff model?: Part 2 — towards a simple and efficient potential
926 evapotranspiration model for rainfall– runoff modelling. *J. Hydrol.* 303, 290–306, 2005.

927 Paeth H., Vogt G., Paxian A., Hertig E., Seubert S., and Jacobeit J.: Quantifying the evidence of climate change
928 in the light of uncertainty exemplified by the Mediterranean hot spot region. *Global and Planetary Change* 151,
929 144-151, 2017.

930 Paton F., Maier H., and Dandy G.: Relative magnitudes of sources of uncertainty in assessing climate change
931 impacts on water supply security for the southern Adelaide water supply system. *Water Resour. Res.* 49(3), 1643–
932 1667, 2013.

933 Perrin C., Michel C., and Andréassian V. Improvement of a parsimonious model for streamflow simulation. *J.*
934 *Hydrol.* 279, 275–289, 2003.

935 Poff N.L., Brown C.M., Grantham T.E., Matthews J.H., Palmer M.A., Spence C.M., Wilby R.L., Haasnoot M.,
936 Mendoza G.F., Dominique K.C., and Baeza A.: Sustainable water management under future uncertainty with eco-
937 engineering decision scaling. *Nature Climate Change* 6(1), 25-34, 2016.

938 Poncelet C., Merz R., Merz B., Parajka J., Oudin L., Andréassian V., and Perrin C.: Process-based interpretation
939 of conceptual hydrological model performance using a multinational catchment set. *Water Resour. Res.* 53, 7247–
940 7268, 2017.

941 Pushpalatha R., Perrin C., Le Moine N., Mathevet T., and Andréassian V. A downward structural sensitivity
942 analysis of hydrological models to improve low-flow simulation. *J. Hydrol.* 411, 66–76, 2011.

943 Prudhomme C., Wilby R.L., Crooks S., Kay A.L. and Reynard N.S.: Scenario-neutral approach to climate change
944 impact studies: Application to flood risk. *J. Hydrol.* 390(3–4), 198-209, 2010.

945 Prudhomme C., Kay A., Crooks S., and Reynard N.: Climate change and river flooding: Climate change and river
946 flooding: Part 1 classifying the sensitivity of British catchments. *Climatic Change* 119, 933-948, 2013a.

947 Prudhomme C., Kay A., Crooks S., and Reynard N. Climate change and river flooding: Part 2 sensitivity
948 characterization for British catchments and example vulnerability assessments. *Climatic Change* 119, 949–964,
949 2013b.

950 Quintana-Seguí P., Le Moigne P., Durand Y., Martin E., Habets F., Baillon M., Canellas C., Franchistéguy L., and
951 Morel S.: Analysis of near-surface atmospheric variables: validation of the safran analysis over France. *J. Appl.*
952 *Meteorol. Clim.* 47, 92–107, 2008.

953 Radnoti G.: Comments on A Spectral Limited-Area Formulation with Time-Dependent Boundary Conditions
954 Applied to the Shallow-Water Equations. *Monthly Weather Review* 123:2, 1995.

955 R Core Team: R: A Language and Environment for Statistical Computing, R Foundation for Statistical Computing,
956 Vienna, Austria, <https://www.R-project.org/>, 2016.

957 Ray P.A. and Brown C.M. *Confronting Climate Uncertainty in Water Resources Planning and Project Design: The*
958 *Decision Tree Framework*. Washington, DC: World Bank, 2015.

959 Rousseeuw P.J. Silhouettes: A graphical aid to the interpretation and validation of cluster analysis. *Journal of*
960 *Computational and Applied Mathematics* 20 (November), 53-65, 1987.

961 Ruf T.: Le projet Aqua Domitia : intérêt et limites. *Pour*, 2012/1(213), 65-74. DOI : 10.3917/pour.213.0065.

962 Samaniego L., Thober S., Kumar R., Wanders N., Rakovec O., Pan M., Zink M., Sheffield J., Wood E.F., and
963 Marx, A.: Anthropogenic warming exacerbates European soil moisture droughts. *Nature Climate Change* 8(5),
964 421-426, <https://doi.org/10.1038/s41558-018-0138-5>, 2018.

965 Sauquet E.: Mapping mean annual river discharges: geostatistical developments for incorporating river network
966 dependencies. *J. Hydrol.* 331, 300–314, 2006.

967 Sauquet E., Gottschalk L., and Krasovskaia I.: Estimating mean monthly runoff at ungauged locations: an
968 application to France. *Hydrology Research* 39(5-6), 403-423, 2008.

969 Sauquet E. and Catalogne C.: Comparison of catchment grouping methods for flow duration curve estimation at
970 ungauged sites in France. *Hydrol. Earth Syst. Sci.* 15, 2421–2435, 2011.

971 Sauquet E., Arama Y., Blanc-Coutagne E., Bouscasse H., Branger F., Braud I., Brun J.-F., Cherel J., Cipriani T.,
972 Datry T., Ducharne A., Hendrickx F., Hingray B., Krowicki F., Le Goff I., Le Lay M., Magand C., Malerbe F.,
973 Mathevet T., Mezghani A., Monteil C., Perrin C., Poulhe P., Rossi A., Samie R., Strosser P., Thirel G., Tilmant
974 F., and Vidal J.-P.: Water allocation and uses in the Durance River basin in the 2050s: Towards new management
975 rules for the main reservoirs?, *La Houille Blanche* 5, 25-31, 2016.

976 Schlef K.E., Steinschneider S., and Brown C.M.: Spatiotemporal Impacts of Climate and Demand on Water Supply
977 in the Apalachicola-Chattahoochee-Flint Basin. *J. Water Resour. Plann. Manage.*, 2018, 144(2): 05017020, 2018.

978 Simonovic S.P.: A new methodology for the assessment of climate change impacts on a watershed scale. *Current*
979 *Science* 98(8), 1047-1055, 2010.

980 Singh R., Wagener T., Crane R., Mann M.E., and Ning L.: A vulnerability driven approach to identify adverse
981 climate and land use change combinations for critical hydrologic indicator thresholds: application to a watershed
982 in Pennsylvania, USA. *Water Resour. Res.* 50(4), 3409–3427, 2014.

983 Skamarock W., Klemp J., Dudhia J., Gill D., Barker D., Wang W., Huang X.-Y., and Duda M.: A description of
984 the advanced research WRF version 3, doi:10.5065/D68S4MVH, 2008.

985 Steinschneider S. and Brown C.M.: A semiparametric multivariate, multisite weather generator with low-
986 frequency variability for use in climate risk assessments, *Water Resour. Res.*, 49, 7205–7220,
987 doi:10.1002/wrcr.20528, 2013.

988 Terray L. and Boé J.: Quantifying 21st-century France climate change and related uncertainties. *Comptes Rendus*
989 *Geoscience*, 345, 136–149, 2013.

990 Therneau T., Atkinson B., and Ripley B. *rpart*: Recursive Partitioning and Regression Trees. R package version
991 4.1-13, <https://CRAN.R-project.org/package=rpart>, 2018.

992 Touma D, Ashfaq M, Nayak M.A., Kao S.-C., Diffenbaugh N.S.: A multi-model and multi-index evaluation of
993 drought characteristics in the 21st century. *J. Hydrol.*, 526, 196-207, 2015

994 Van Loon A.F., Gleeson T., Clark J., Van Dijk A.I.J.M., Stahl K., Hannaford J., Di Baldassarre G., Teuling A.J.,
995 Tallaksen L.M., Uijlenhoet R., Hannah D.M., Sheffield J., Svoboda M., Verbeiren B., Wagener T., Rangelcroft S.,
996 Wanders N., and Van Lanen H.A.J.: Drought in the Anthropocene, *Nature Geoscience*, 9, 89-91, 2016.

997 Taylor K.E., Stouffer R.J., and Meehl G.A.: An overview of CMIP5 and the experiment design. *Bull. Am.*
998 *Meteorol. Soc.* 93(4), 485-498, 2012.

999 Valéry A., Andréassian V., and Perrin C.: 'As simple as possible but not simple': What is useful in a temperature-
1000 based snow-accounting routine? Part 2 - Sensitivity analysis of the Cemaneige snow accounting routine on 380
1001 catchments. *J. Hydrol.* 517, 1176–1187, 2014.

1002 Vidal J.-P., Martin E., Franchistéguy L., Baillon M, and Soubeyrou J.-M.: A 50-year high-resolution atmospheric
1003 reanalysis over France with the Safran system. *Int. J. Clim.* 30, 1627–1644, 2010.

1004 Vidal J.-P., Hingray B., Magand C., Sauquet E., and Ducharne A.: Hierarchy of climate and hydrological
1005 uncertainties in transient low-flow projections. *Hydrol. Earth Syst. Sci.* 20, 3651–3672, 2016.

1006 Ward J. Jr.: Hierarchical grouping to optimize an objective function. *Journal of the American Statistical*
1007 *Association* 58(301), 236-44, 1963.

1008 Whateley S., Steinschneider S., and Brown C.M.: A climate change range-based method for estimating robustness
1009 for water resources supply. *Water Resour. Res.* 50, 8944–8961, 2014.

1010 Weiß M.: Future water availability in selected European catchments: a probabilistic assessment of seasonal flows
1011 under the IPCC A1B emission scenario using response surfaces. *Nat Hazards Earth Syst Sci* 11:2163–2171, 2011.

1012 Wetterhall F., Graham L.P., Andréasson J., Rosberg J., and Yang W. Using ensemble climate projections to assess
1013 probabilistic hydrological change in the nordic region. *Natural Hazards and Earth System Sciences* 11, 2295–2306,
1014 2011.

1015 Wickham H.: *ggplot2: Elegant Graphics for Data Analysis*, Springer-Verlag New York, <http://ggplot2.org>, 2009.

1016 Wickham H. and Francois R. *dplyr: A Grammar of Data Manipulation*. R package version 0.4.3, [https://CRAN.R-](https://CRAN.R-project.org/package=dplyr)
1017 [project.org/package=dplyr](https://CRAN.R-project.org/package=dplyr), 2015.

1018 Wickham H.: scales: Scale Functions for Visualization. R package version 0.4.0, [https://CRAN.R-](https://CRAN.R-project.org/package=scales)
1019 [project.org/package=scales](https://CRAN.R-project.org/package=scales), 2016.

1020 Wickham H.: stringr: Simple, Consistent Wrappers for Common String Operations. R package version 1.2.0,
1021 <https://CRAN.R-project.org/package=stringr>, 2017.

1022 Wickham H.: stringr: Simple, Consistent Wrappers for Common String Operations. R package version 1.2.0.
1023 <https://CRAN.R-project.org/package=stringr>, 2017.

1024 Zambrano-Bigiarini M.: hydroTSM: Time series management, analysis and interpolation for hydrological
1025 modelling. R package version 0.4-2-1. <https://CRAN.R-project.org/package=hydroTSM>, 2014.

1026 Zeileis A. and Grothendieck G.: zoo: S3 Infrastructure for Regular and Irregular Time Series. Journal of Statistical
1027 Software, 14(6), 1-27. doi:10.18637/jss.v014.i06, 2005.

1028

N°	River basin	Department (department number)	Station number	Elevation (m.a.s.l.)	Area (km ²)	Regime class	NSE _{LOG}	KGE _{SQRT}
1	Ouche	Côte d'Or (21)	U1324010	243	651	6	0.84	0.94
2	Bourbre	Isère (38)	V1774010	202	703	1	0.85	0.92
3	Roizonne	Isère (38)	W2335210	936	71.6	11	0.71	0.84
4	Bonne	Isère (38)	W2314010	770	143	12	0.80	0.91
5	Buëch	Hautes-Alpes (05)	X1034020	662	723	9	0.84	0.93
6	Drôme	Drôme (26)	V4214010	530	194	3	0.81	0.89
7	Drôme	Drôme (26)	V4264010	263	1150	9	0.85	0.88
8	Roubion	Drôme(26)	V4414010	264	186	9	0.83	0.93
9	Lot	Lozère (48)	O7041510	663	465	3	0.88	0.94
10	Tarn	Lozère (48)	O3011010	905	67	8	0.73	0.90
11	Tarn	Lozère (48)	O3031010	565	189	9	0.81	0.91
12	Hérault	Hérault (34)	Y2102010	126	912	8	0.83	0.88
13	Asse	Alpes de Haute-Provence (04)	X1424010	605	375	9	0.80	0.86
14	Caramy	Var (83)	Y5105010	172	215	2	0.85	0.94
15	Argens	Var (83)	Y5032010	175	485	2	0.80	0.92

1030 **Table 1: Main characteristics of the 15 catchments used for validation of water restriction simulations. Station number**
1031 **refers to the catchment number in the HYDRO database and regime class to the classification suggested by Sauquet *et***
1032 ***al.* (2008) with a gradient from Class 1- pluvial fed regime moderately contrasted to Class 12- snowmelt fed regime.**

1033

Data source	Representative Concentration Pathway			Reference
	RCP2.6	RCP4.5	RCP8.5	
ALADIN	A	A	NA	Bubnová et al. (1995). Radnoti (1995)
First quartile, median and last quartile of the ensemble EURO-CORDEX results	NA	A	A	Jacob et al. (2014)
WRF	NA	A	NA	Skamarock et al. (2008)

1034 **Table 2: Regional climate projections available in the DRIAS portal (A: available; NA: not available).**

1035

Level	Name	Water restriction							
		Recreational	Vehicle washing	Lawn watering	Swimming-pool filling	Urban washing	Irrigation	Industry	Drinking water and sanitation
0	Vigilance	×	×	×	×	×			
1	Alert	×	×	×	×	×	×	×	
2	Reinforced alert	×	×	×	×	×	×	×	
3	Crisis	×	×	×	×	×	×	×	×

1036 **Table 3: Uses affected by water restriction according to the drought severity**

1037

WR* event	WR level ≥ 1 (Benchmark)		
	<i>Yes</i>	<i>No</i>	
WR level ≥ 1 (Prediction)	<i>Yes</i>	hits	false alarms
	<i>No</i>	misses	correct negatives

1038 **Table 4: Contingency table for legally-binding restriction (WR*).**

1039

	<i>Sd</i>	Period		
		AMJJASO	JASO	MAMJ
Argens River basin (Class 1)	median	1.59	1.65	0.19
	max	3.32	3.69	1.21
Ouche River basin (Class 2)	median	0.63	0.78	1.10
	max	1.03	1.52	1.99
Roizonne River basin (Class 4)	median	1.12	1.32	0.64
	max	1.98	2.49	0.91
All	median	0.69	0.80	0.70
	max	1.45	1.70	1.24
Class 1	median	1.16	1.24	0.25
	max	2.70	2.96	1.17
Class 2	median	0.72	0.85	0.89
	max	1.45	1.81	1.43
Class 3	median	0.41	0.49	0.64
	max	0.88	0.97	1.06
Class 4	median	0.91	1.14	0.81
	max	1.78	2.15	1.28

1040 **Table 5: Summary statistics for standard deviation *Sd* of the grid for different axes.**

1041

Component of the river flow regime	Hydrological indices
Severity	Flow exceeded 95% of the time (Q_{95})
	Annual minimum 10-day daily mean low flow with a 5-year recurrence interval Annual maximum deficit below threshold Q_{95} exceeded 20% of time
Duration	Annual maximum maximal duration of the continuous sequence of zero flow within the year, exceeded on average every five years (D_{80}). Maximum duration of consecutive zero flows (D) are sampled by block maxima approach and D_{80} is defined as the empirical 80th percentile of cumulative distribution function of D
	Seasonal recession time scales (DT and $Drec$). This duration is based on the hydrograph defined by the 1-day and 30-day moving average of the 365 long term mean daily discharges, $d=1, \dots, 365$ (Q_d and Q_{30d} , respectively). $Drec$ is defined by the time lapse between the median Q_{d50} and the 90th quantile Q_{d90} of Q_d on the falling limb of the hydrograph defined by Q_{30d} and $DT = \ln(Q_{d50}/Q_{d90})/Drec$
Rate of Change	Ratio Q_{95}/Q_{50}
	Concavity index derived from flow duration curve $(Q_{10} - Q_{99})/(Q_1 - Q_{99})$ (Sauquet and Catalogne 2011). This descriptor is a dimensionless measure of the contrast between low-flow and high-flow regimes derived from quantiles of the flow duration curve
	Baseflow index (BFI). BFI is a measure of the proportion of the baseflow component to the total river flow, calculated by the separation algorithm separation suggested by Lyne and Hollick (1979)
	Class of river flow regime based on average monthly runoff pattern defined by Sauquet <i>et al.</i> (2008) (between 1 and 12)
Frequency	Seasonality ratio (SR) $SR = Q_{95_{AMJJASON}}/Q_{95_{DJFM}}$ ($SR > 1$ for mountainous catchment) with $Q_{95_{AMJJASON}}$ and $Q_{95_{DJFM}}$ computed on seasonal flow duration curves
	Proportion of years with at least one value below Q_{95}
Timing	Mean day of first occurrence of flow below Q_{95}
	Mean and dispersion of the occurrence of flows below Q_{95} within the year (θ and r , $r\sin(\theta)$ and $r\cos(\theta)$). These two variables are circular statistics. Each day i with zero flow is converted into an angular (t_i) and represented by a unit vector with rectangular coordinates ($\cos(t_i)$; $\sin(t_i)$). The mean of the cosines and sines defines a representative vector. The value for θ is obtained by calculating the inverse tangent of the angle of the mean vector and the norm of the mean vector provides a measure of the regularity in the dates (a value close to one indicates a high concentration around θ while a value close to zero indicates no seasonality)

1043 **Table 6: Hydrological metrics considered to investigate similarity in CART.**

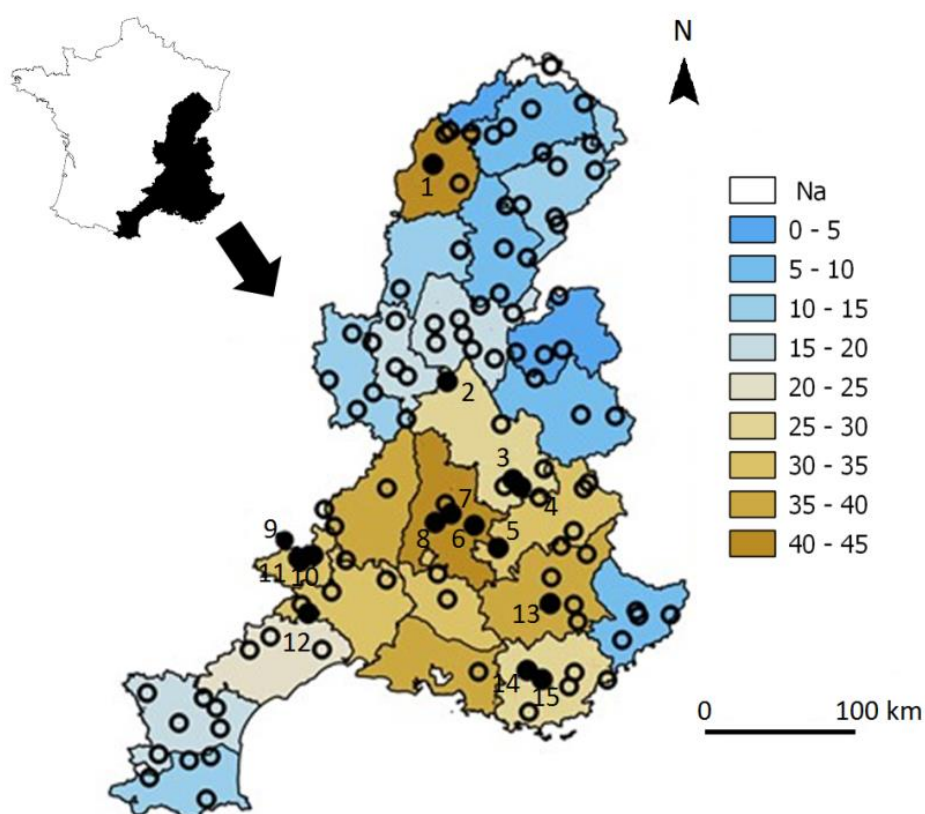
1045

Class		Number of catchments (with agricultural disaster status)	Mean $\Delta WR^*(2011)$ (with agricultural disaster status) ($\times 10$ days)	Vulnerability index VI (%)		
				2021-2050	2041-2070	2071-2100
1	All	15 (2)	-1.2 (-2.3)	6.1	11.5	6.7
2	All	44 (22)	5.0 (7.1)	6.4	11.8	21.6
	N	25 (18)	6.1 (6.2)	0	0	13
	S	19 (4)	3.4 (11.3)	14.8	27.3	32.9
3	All	38 (13)	5.4 (8.7)	1.7	4.5	7.9
	N-E	25 (4)	3.7 (3.8)	0.4	0	4.5
	S-W	13 (9)	8.5 (10.8)	4.19	13.3	14.4
4	All	9 (3)	0 (-0.7)	18.2	45.4	47.2
All		106 (40)	3.8 (6.6)	5.8	12	16.7

1046 **Table 7: Summary statistics for the mean anomaly $\Delta WR^*(2011)$ and for the measure of vulnerability VI estimated at**
 1047 **the regional scale.**

1048

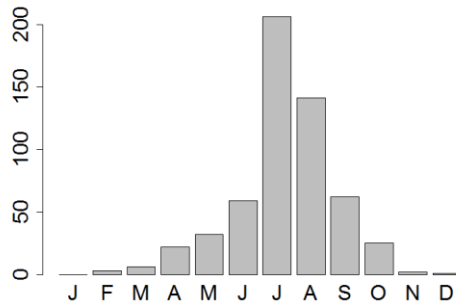
1049



1050

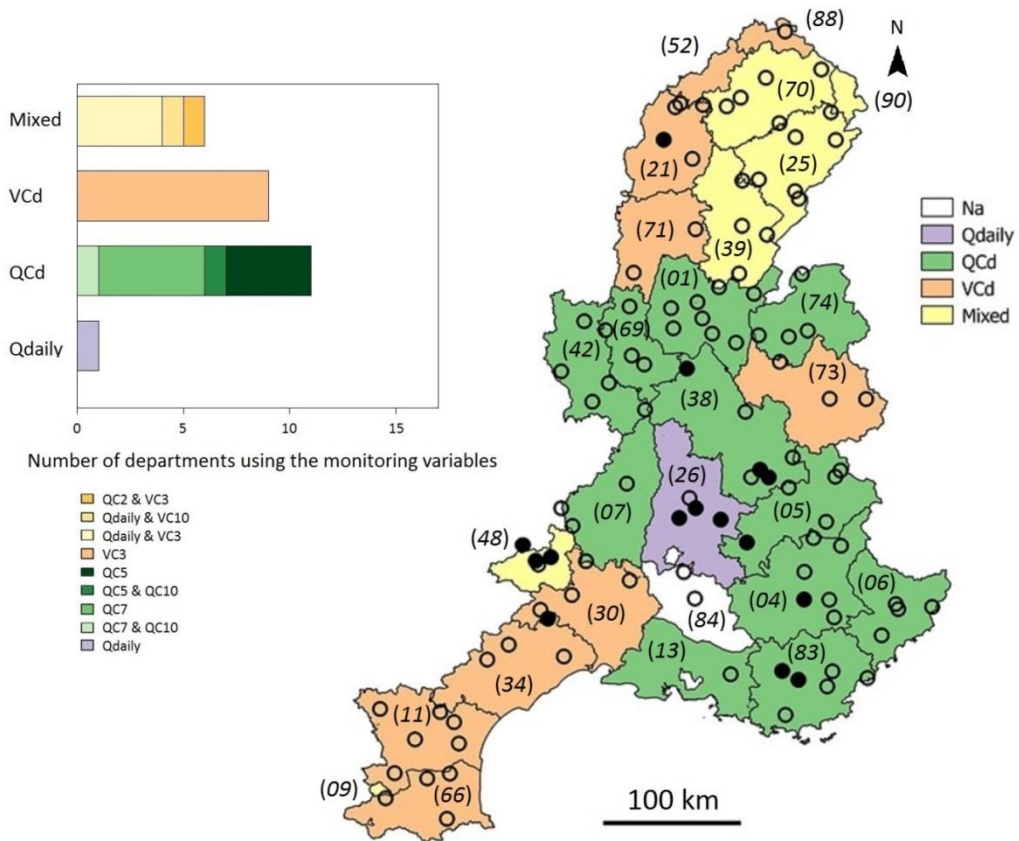
1051 **Figure 1: The Rhône-Méditerranée water district, the total number of WR decisions stated by department over the**
 1052 **period 2005-2016 and the gauged catchments \bigcirc where WR decisions are simulated (\bullet denotes the subset of the 15**
 1053 **catchments used for evaluation purposes and the figures are the related ranks presented in Table 1).**

1054



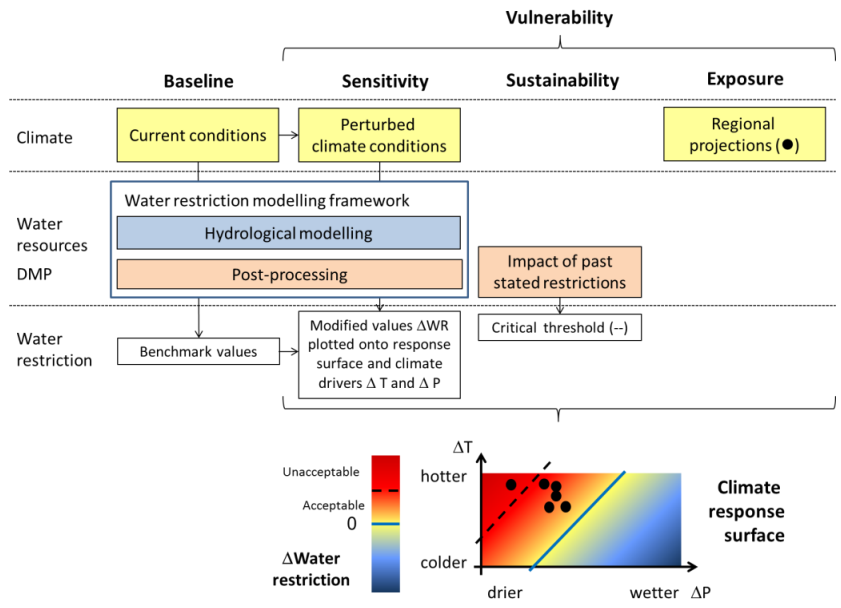
1055

1056 **Figure 2: Total number of stated WR decisions over the RM district per month over the period 2005-2016.**



1057

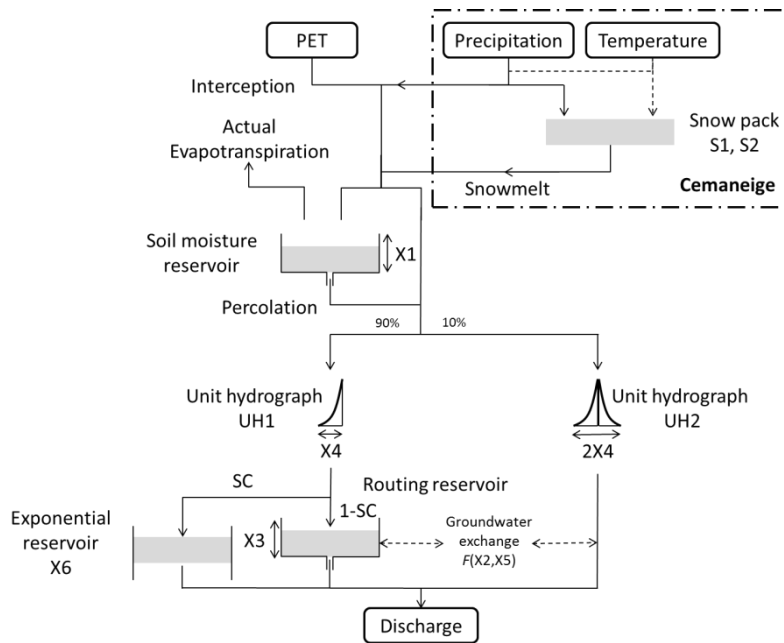
1058 **Figure 3: Low-flow monitoring variables used in the current drought management plans. *Qdaily* denotes daily**
 1059 **streamflow, *QCd* the *d*-day maximum discharge; *VCd* the *d*-day mean discharge and *Mixed* refers to combinations of**
 1060 **the aforementioned variables. Department codes are given into brackets.**



1061

1062 **Figure 4: Schematic framework of the developed approach to assess the vulnerability of the DMPs under climate**
 1063 **change.**

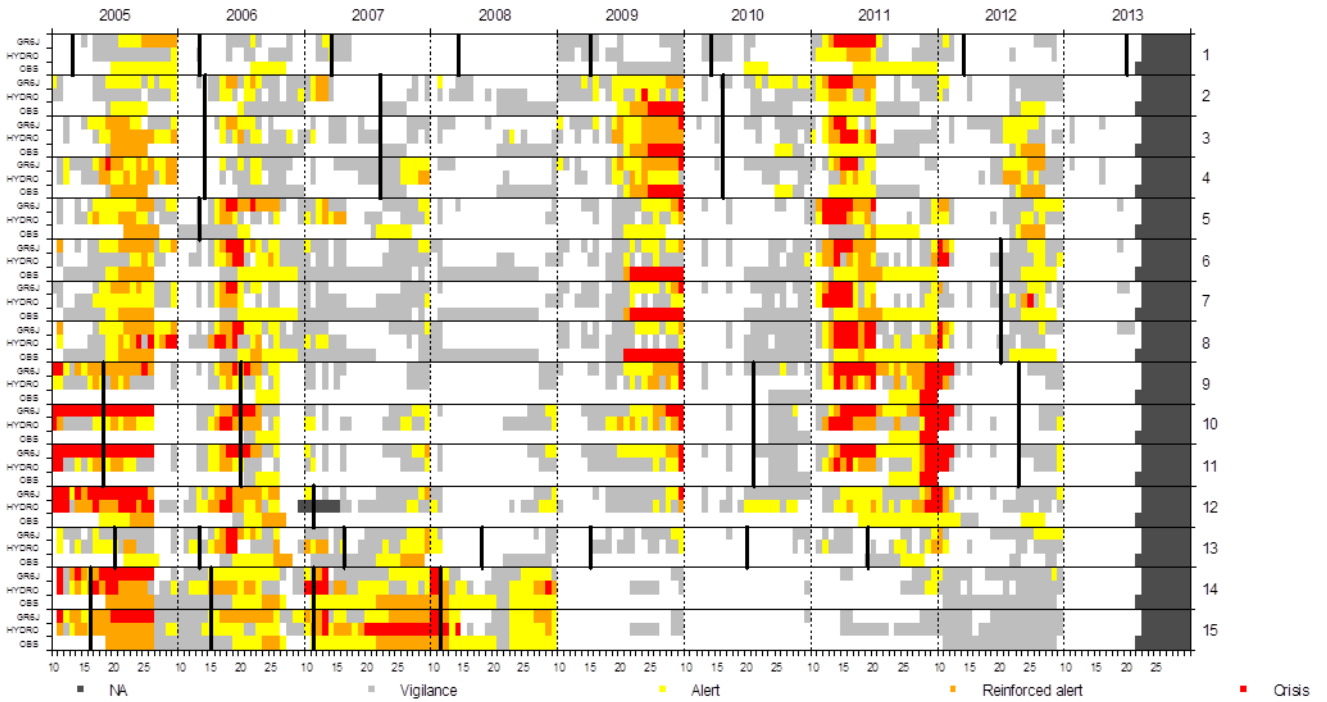
1064



1065

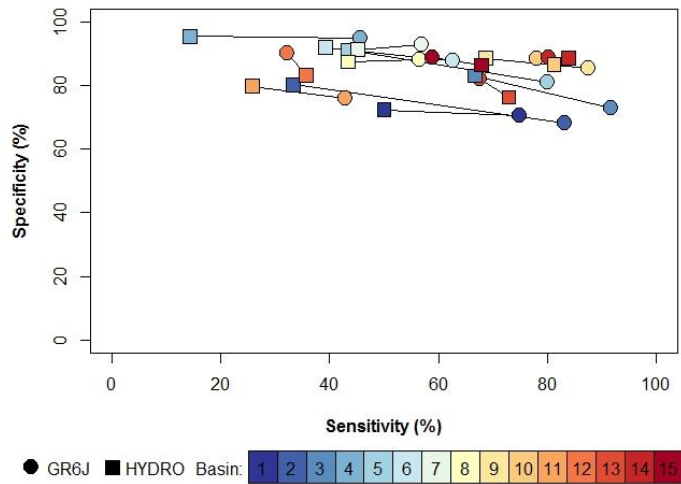
1066 **Figure 5: Schematic of the rainfall-runoff Model GR6J combined with the CemaNeige snowmelt runoff component**
 1067 **(after Pushpalatha *et al.* 2011).**

1068



1069

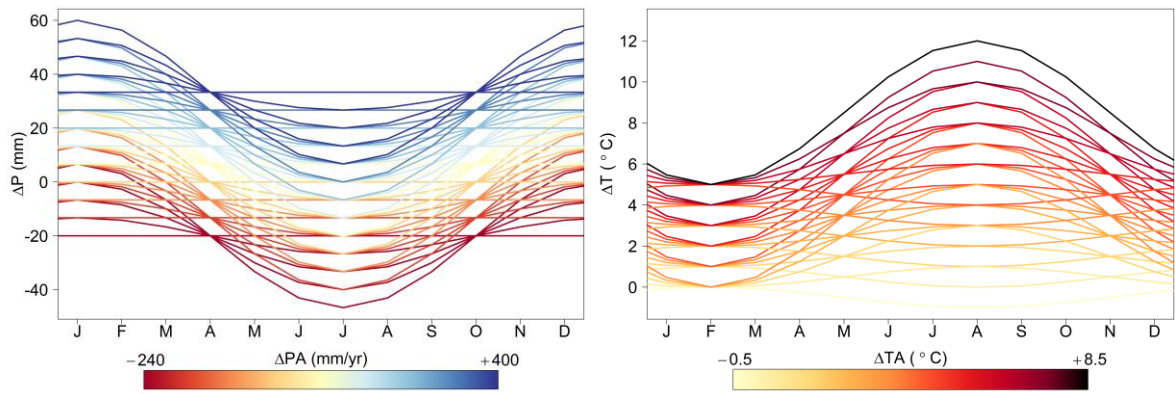
1070 **Figure 6: Observed and simulated water restriction levels considering the two sources of discharge data GR6J and**
 1071 **HYDRO for each of the 15 evaluation catchments (Table 1). The x-abscissa is divided into ten-day periods for each year**
 1072 **spanning the period April-to-October. Black segments identify updated DMPs.**



1073

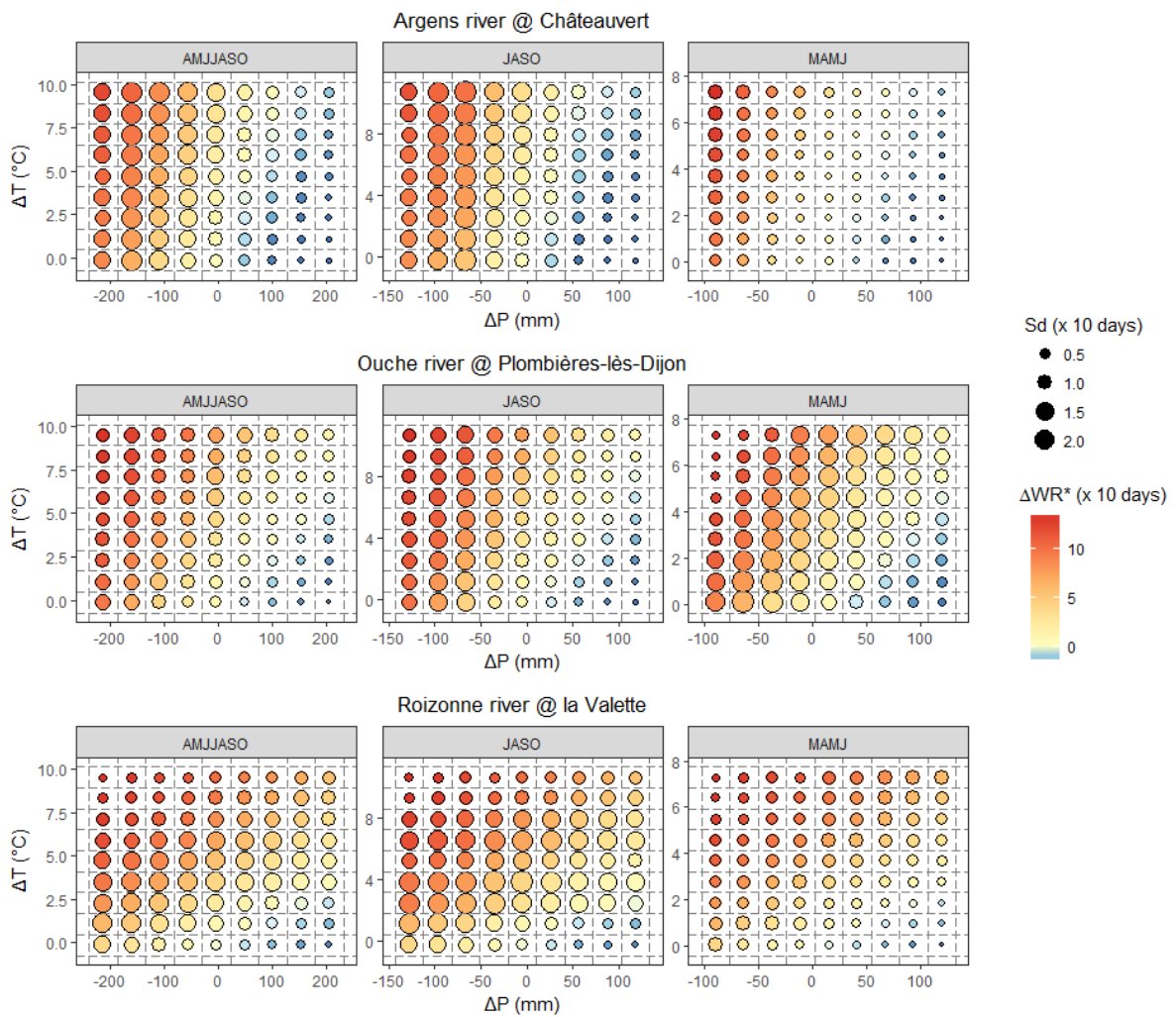
1074 **Figure 7: Skill scores obtained for the WR level model over the period 2005-2013. Each segment is related to one of the**
 1075 **15 catchments listed in Table 2. The endpoints refer to the source of discharge data (GR6J or HYDRO).**

1076



1077

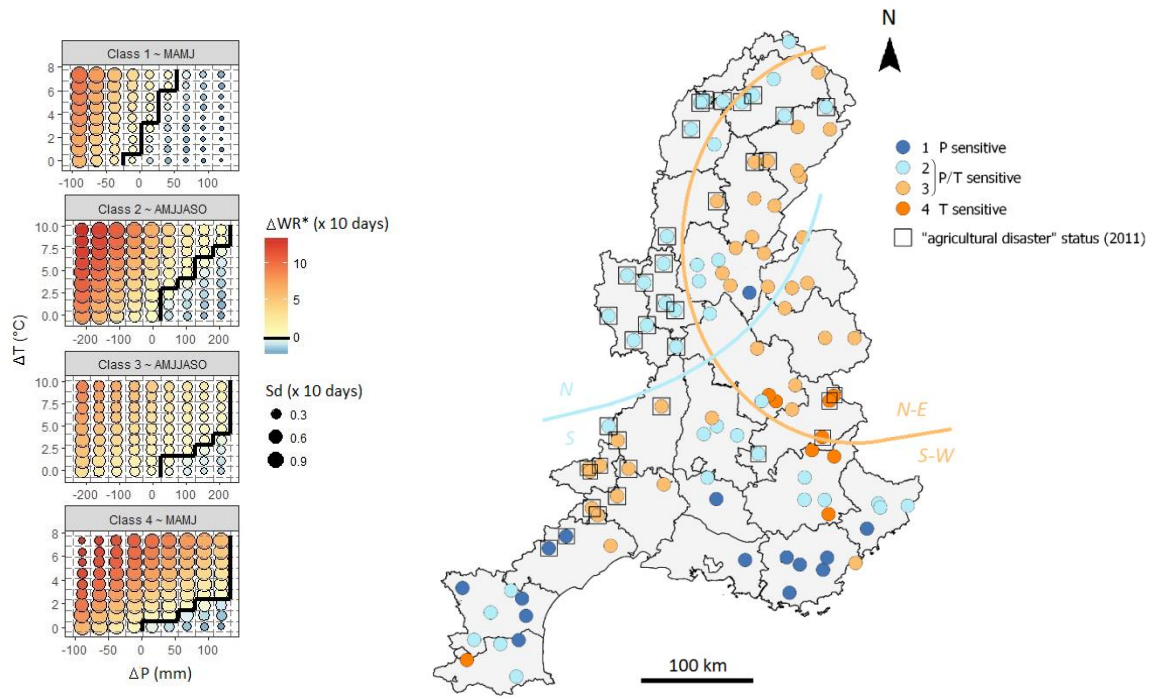
1078 **Figure 8: Monthly perturbation factors ΔP and ΔT associated with the climate sensitivity domain. The color of the line**
 1079 **is related to the intensity of the annual change ΔPA and ΔTA .**



1080

1081 **Figure 9: Climate response surface of legally-binding water restrictions level anomalies ΔWR^* for the Argens, Ouche**
 1082 **and Roizonne River basins. Each graph is obtained considering changes in mean precipitation ΔP and temperature ΔT**
 1083 **over a specific period as x- and y-axis.**

1084

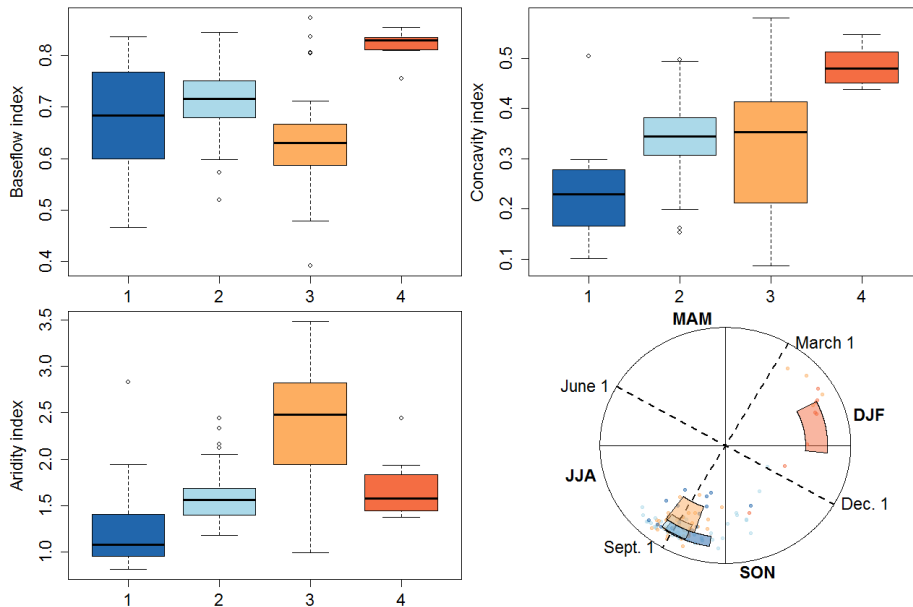


1085

1086 **Figure 10: Results of the hierarchical cluster analysis applied to the climate response surface WR* level anomalies**

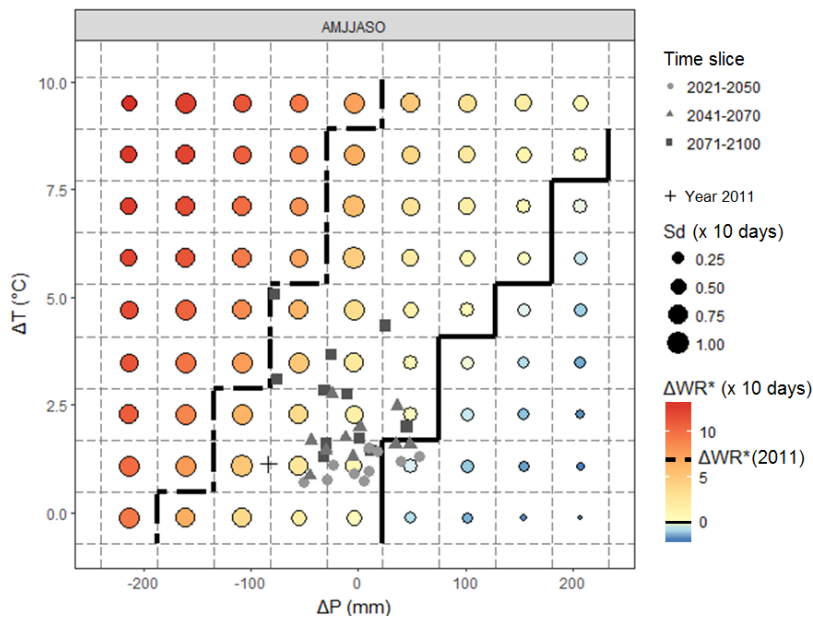
1087 **ΔWR^***

1088



1089

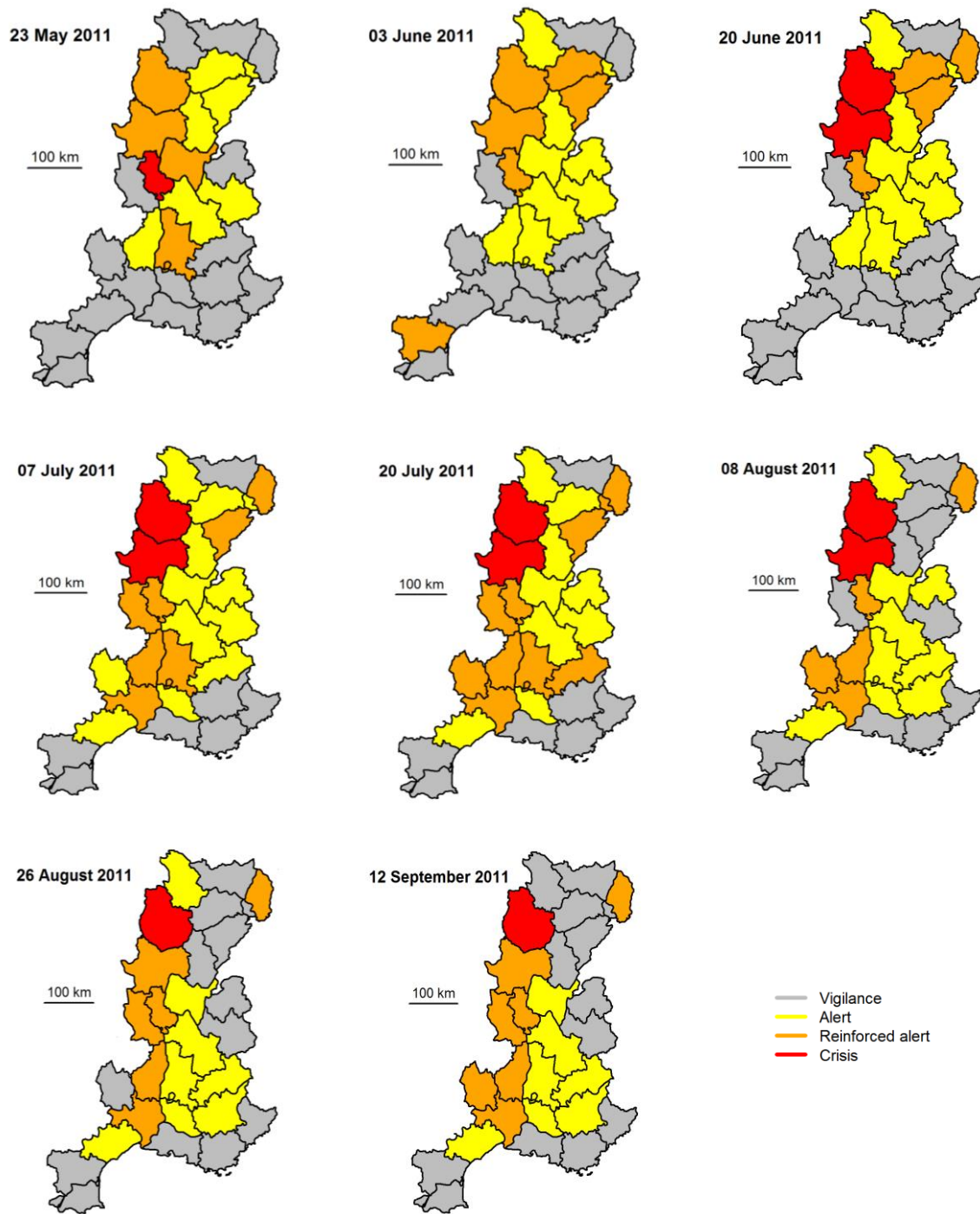
1090 **Figure 11: Statistical distribution of the discriminating factors identified by the CART algorithm (top level, top left and**
 1091 **bottom left) and the mean timing θ of daily discharge below $Q95$ and its dispersion r (bottom right). The boxplots are**
 1092 **defined by the first quartile, the median and the third quartile. The whiskers extend to 1.5 of the interquartile range;**
 1093 **open circles indicate outliers. The color is associated to the membership to one class and the name of the class is given**
 1094 **along the x-axis. The colored areas in the lower right figure are defined by the first quartile and the third quartile of r**
 1095 **and θ . Each dot is related to one gauged basin. The dotted lines indicate the start of four meteorological seasons.**



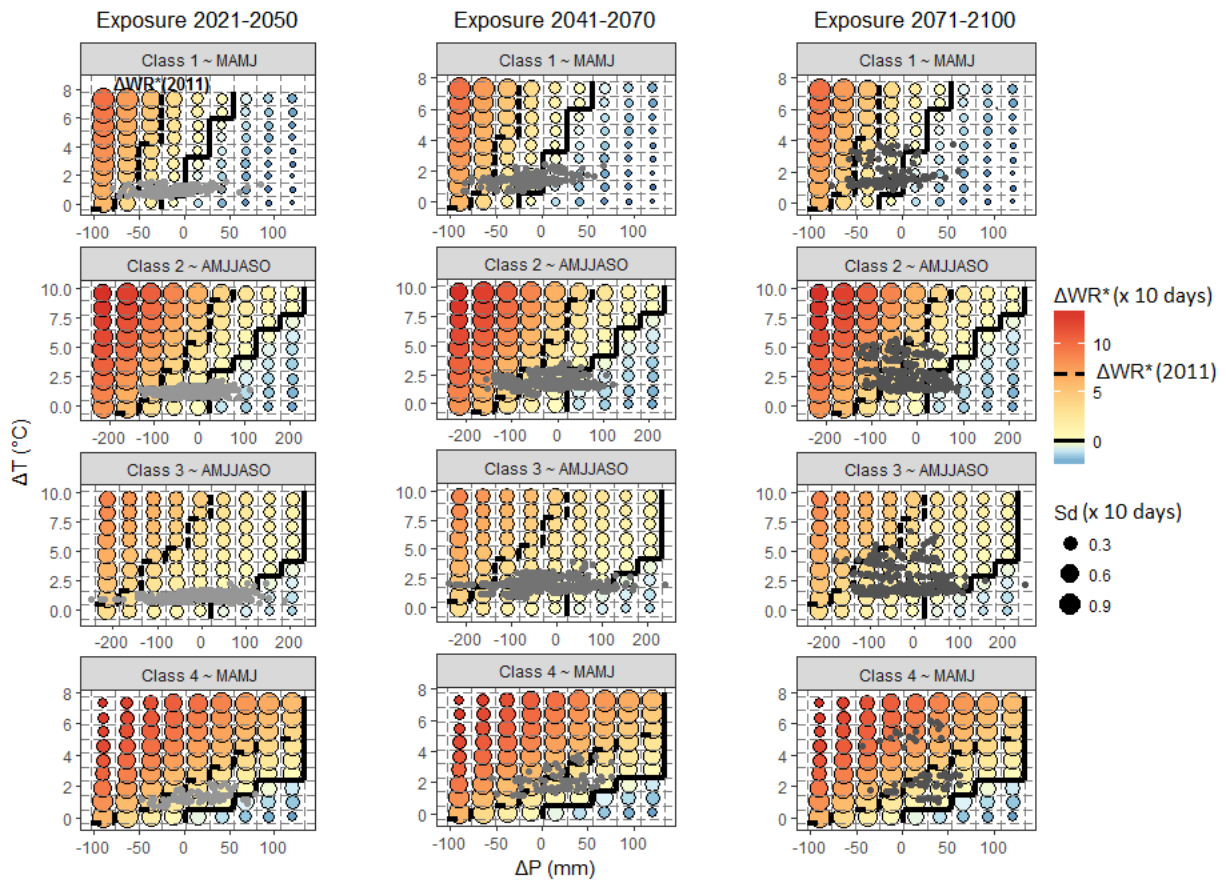
1096

1097 **Figure 12: Climate response surface of legally-binding water restrictions level anomalies ΔWR^* for the Ouche River**
 1098 **basin including both exposure and performance characterizations.**

1099



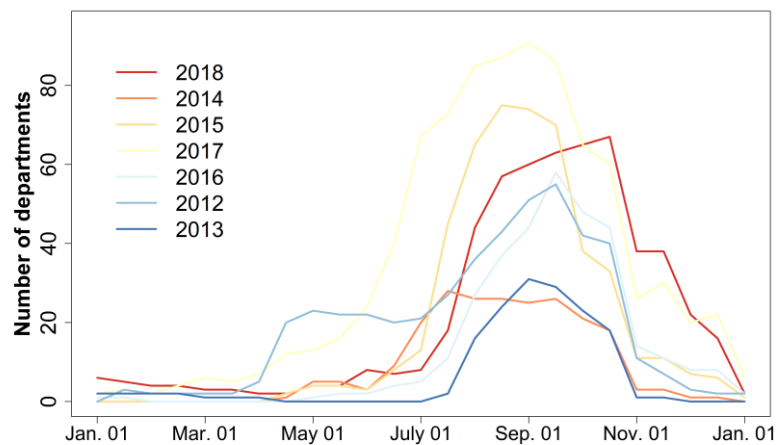
1101 **Figure 13: Most severe water restriction level adopted at the department-level scale for several dates between May and**
 1102 **September 2011 (Source: French ministry of Ecology)**



1104

1105 **Figure 14: Representative climate response surfaces for each class including both exposure and performance**
 1106 **characterizations.**

1107



1108

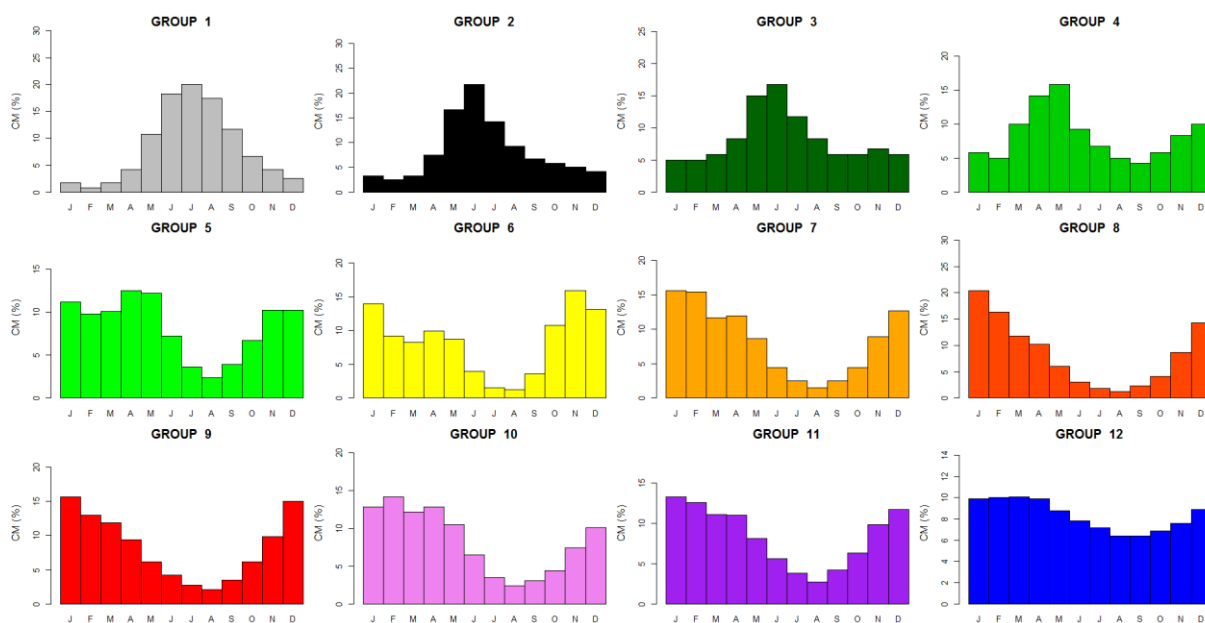
1109 **Figure 15: Number of departments with at least one sub-catchment with WR level ≥ 1 . The color of the curves is**
 1110 **associated to the annually averaged air temperature rank for France (from red to blue for the warmest (2018) to the**
 1111 **coldest year (2013)) (Sources: MétéoFrance, French ministry of Ecology).**

1112

1113 **Appendix A: Classification of river flow regime for France**

1114 Sauquet *et al.* (2008) have defined a classification based on the mean monthly runoff pattern (Fig. A1) and a
 1115 map has been published showing the assignment to one class along the main river network. The twelve
 1116 dimensionless coefficients *CM* are the twelve values of mean monthly runoff (mm) divided by the mean annual
 1117 runoff).

1118 Groups 1 to 6 are pluvial river flow regimes. The six groups mainly differ by the contrast between the maximum
 1119 and the minimum of the monthly discharges. Nearly uniform flows through most of the year (Group 1) are found
 1120 where large aquifers moderate flows whereas Group 6 is characterized by very low flow in summer, reflecting the
 1121 lack of deep groundwater storages in the catchment. Group 7 is representative of Mediterranean river flow regimes
 1122 where small rivers basins experience hot and dry summers and intense rainy events in autumn. Their runoff pattern
 1123 therefore exhibits severe low flow in summer and high flow in November. In mountainous areas, uppermost basins
 1124 display snowmelt-fed regimes (Groups 10, 11 and 12). The lower the outlet is, the lower the contributions of
 1125 snowmelt to runoff. Groups 8 to 9 are in the transition regime. The seasonal variation of streamflow is affected as
 1126 much by precipitation timing as by air temperature and topographic influences (on snowpack formation and
 1127 snowmelt timing). Typically, high flows are observed in spring.



1128
 1129 **Figure A1 : Reference dimensionless hydrographs representative of the classification of river flow regime for France**
 1130 **(after Sauquet *et al.* 2008)**